Electronic Supplementary Material (ESI) for Dalton Transactions.
This journal is © The Royal Society of Chemistry 2019

Supporting Information

Dinuclear Zwitterionic Silver(I) and Gold(I) Complexes Bearing 2,2-Acetate-Bridged Bisimidazolylidene Ligands

Bruno Dominelli,[a] Gerri M. Roberts,[a] Christian Jandl,[a] Pauline J. Fischer,[a] Robert M. Reich,[a] Alexander Pöthig,[a] João D.G. Correia,[b] Fritz E. Kühn[a]*

[a] Molecular Catalysis, Catalysis Research Center and Department of Chemistry, Technische Universität München, Lichtenbergstr. 4, 85747 Garching bei München, Germany.

[b] Centro de Ciências e Tecnologias Nucleares, Departamento de Engenharia e Ciências Nucleares, Instituto Superior Técnico, Universidade de Lisboa, Campus Tecnológico e Nuclear, Estrada Nacional Nº 10 (km 139,7), 2695-066 Bobadela LRS, Portugal

* Corresponding Author: E-mail: fritz.kuehn@ch.tum.de;

Table of Contents

1. General

All chemicals and solvents were purchased from common commercial suppliers and used without further purification. **L_a-H_2-Br** and **L_b-H_2-Br** has been synthesized according to the respective literature procedure.[1, 2] The corresponding zwitterionic dinuclear silver(I)- and gold(I)-bis(NHC) complexes, have been obtained by treatment of the bisimidazolium salts with Ag_2O and further transmetalation to a gold(I)-precursor.[3, 4] **^{1}H NMR** and **^{13}C-NMR** spectra were recorded on a *Bruker AV400US* with broad band probe and a gradient coil (^{1}H-NMR, 400.13 MHz, ^{13}C-NMR, 100.53 MHz) and a *Bruker* DRX-400 spectrometer with broad band probe (^{1}H-NMR 400.13 MHz; ^{13}C-NMR 100.61 MHz). All ^{13}C-Cryo-NMR spectra were recorded on a *Bruker AV500C QNP Cryo probe*. Chemical shifts (δ) are reported relative to the residual signal of the deuterated solvent. **Elemental analyses** were carried out by the microanalytical laboratory at the Technical University of Munich. **ESI mass spectrometry** was performed at *Thermo Scientific* LCQ Fleet Spectrometer with a time-of-flight analyser for mass detection. As eluent a mixture of acetonitrile and formic acid (0.1 Vol.%) was used as positive ionization source. FT-IR spectroscopy was measured on PerkinElmer Frontier™ FT-IR spectrometer equipped with an ATR plate with combined ZnSe/Diamond-crystal and a spectral range from 4000 – 650 cm^{-1}. Data were collected on a single crystal x-ray diffractometer equipped with a CCD detector (APEX II, κ-CCD), a rotating anode FR591 and a Montel mirror optic using the APEX2 software package (**L_a-H_2-PF_6** and **$Au_2(L_a)_2$**) or a single crystal x-ray diffractometer equipped with a CMOS detector (Bruker APEX III, κ-CMOS), an IMS microsource with MoK_α radiation (λ = 0.71073 Å) and a Helios optic using the APEX3 software package (**$Ag_2(L_a)_2$** and **$Ag_2(L_b)_2$**).[5] Measurements was performed on single crystals coated with perfluorinated ether. The crystals were fixed on top of a glass fibre or kapton micro sampler and frozen under a stream of cold nitrogen. A matrix scan was used to determine the initial lattice parameters. Reflections were corrected for Lorentz and polarisation effects, scan speed, and background using SAINT.[6] Absorption correction, including odd and even ordered spherical harmonics was performed using SADABS or TWINABS.[7] Space group assignment was based upon systematic absences, E statistics, and successful refinement of the structure. The structures were solved using SHELXS or SHELXT with the aid of successive difference Fourier maps, and were refined against all data using SHELXL in conjunction with SHELXLE.[8,9,10] Hydrogen atoms were calculated in ideal positions as follows: Methyl hydrogen atoms were refined as part of rigid rotating groups, with a C–H distance of 0.98 Å and $U_{iso(H)}$ = 1.5·$U_{eq(C)}$. Other H atoms were placed in calculated positions and refined using a riding model, with methylene and aromatic C–H distances of 0.99 Å and 0.95 Å, respectively, and other C–H distances of 1.00 Å, all with $U_{iso(H)}$ = 1.2·$U_{eq(C)}$. Non-hydrogen atoms were refined with anisotropic displacement parameters. Full-matrix least-squares refinements were carried out by minimizing $\Sigma w(F_o^2 - F_c^2)^2$ with the SHELXL weighting scheme.[8] Neutral atom scattering factors for all atoms and anomalous dispersion corrections for the non-hydrogen atoms were taken from *International Tables for Crystallography*.[11] A split layer refinement was used for disordered groups and additional SIMU, DELU, RIGU, ISOR and SAME restraints were used, if necessary. The unit cell of **$Ag_2(L_a)_2$** contains 16 disordered water molecules and the unit cell of **$Ag_2(L_b)_2$** contains 4 ethanol molecules, 3 of which were

disordered over special positions. In both cases the disordered solvent molecules were treated as a diffuse contribution to the overall scattering without specific atom positions using the PLATON/SQUEEZE procedure.[12] Images of the crystal structures were generated with PLATON and Mercury.[13, 14] CCDC 1942899-1942902 contains the supplementary crystallographic data for this paper. These data are provided free of charge by The Cambridge Crystallographic Data Centre.

2. ^{1}H and ^{13}C NMR spectra

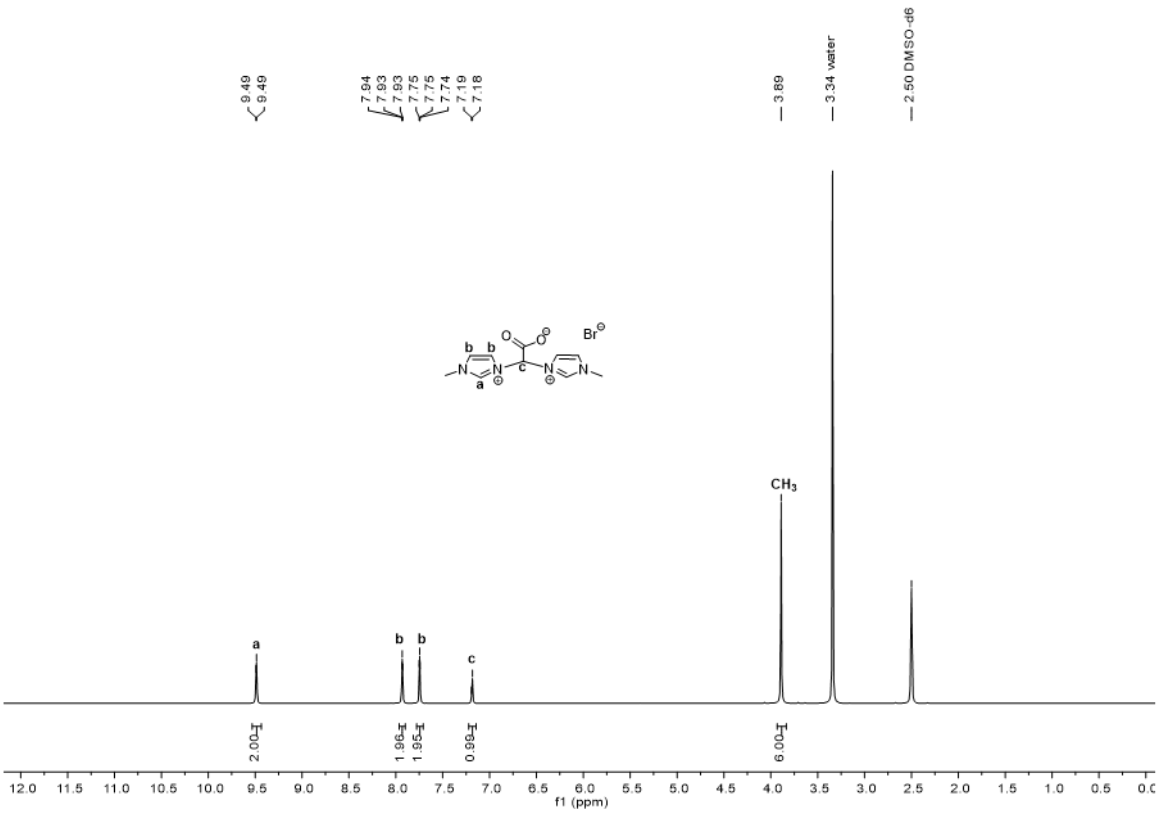

SI-Figure 1: ^{1}H NMR spectrum of **L_a-H_2-Br** in DMSO-d_6 at room temperature.

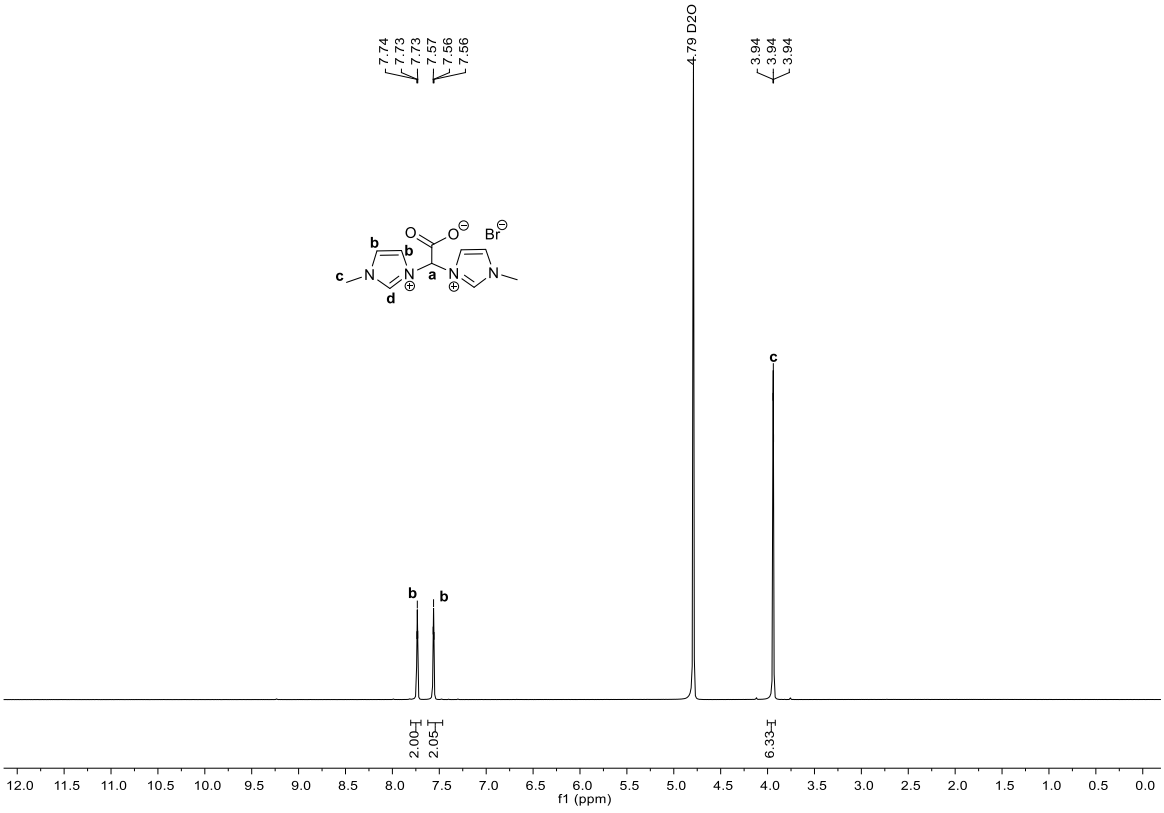

SI-Figure 2: ^{1}H NMR spectrum of **L_a-H_2-Br** in D_2O at room temperature.

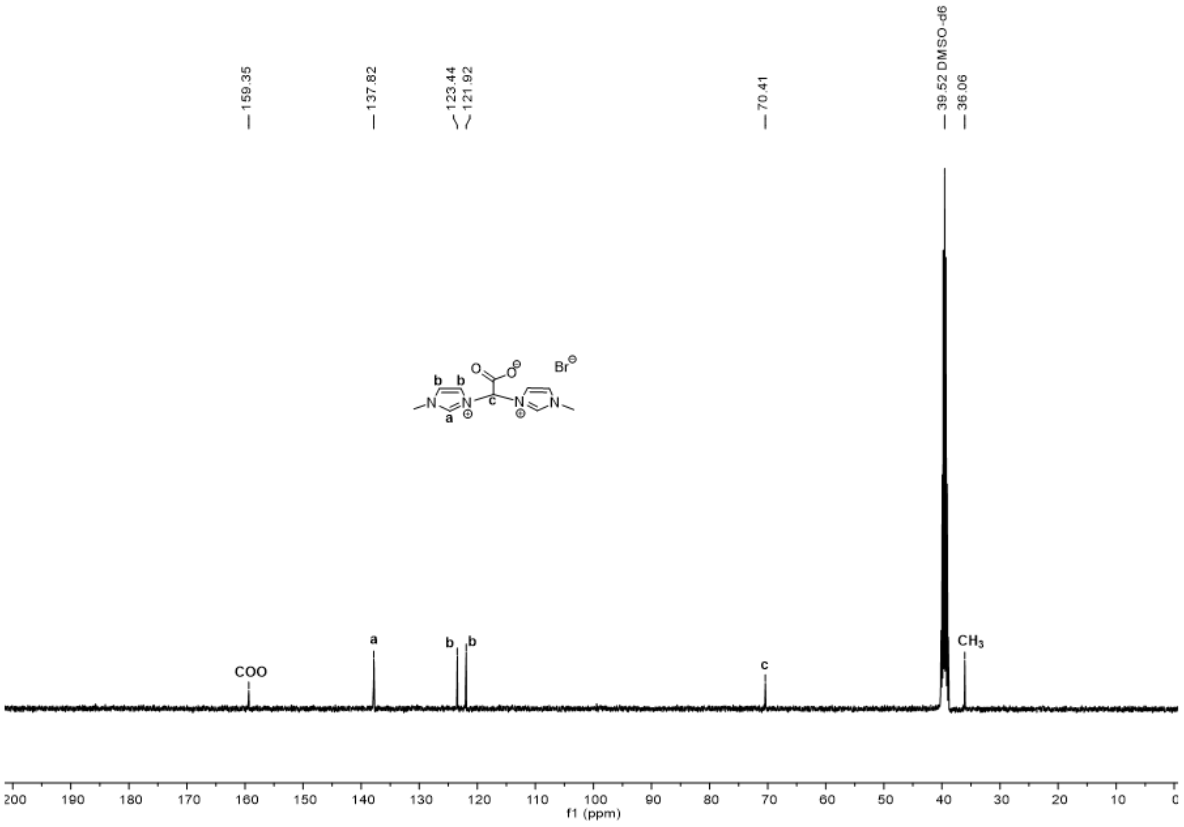

SI-Figure 3: ^{13}C NMR spectrum of **L_a-H_2-Br** in DMSO-d_6 at room temperature.

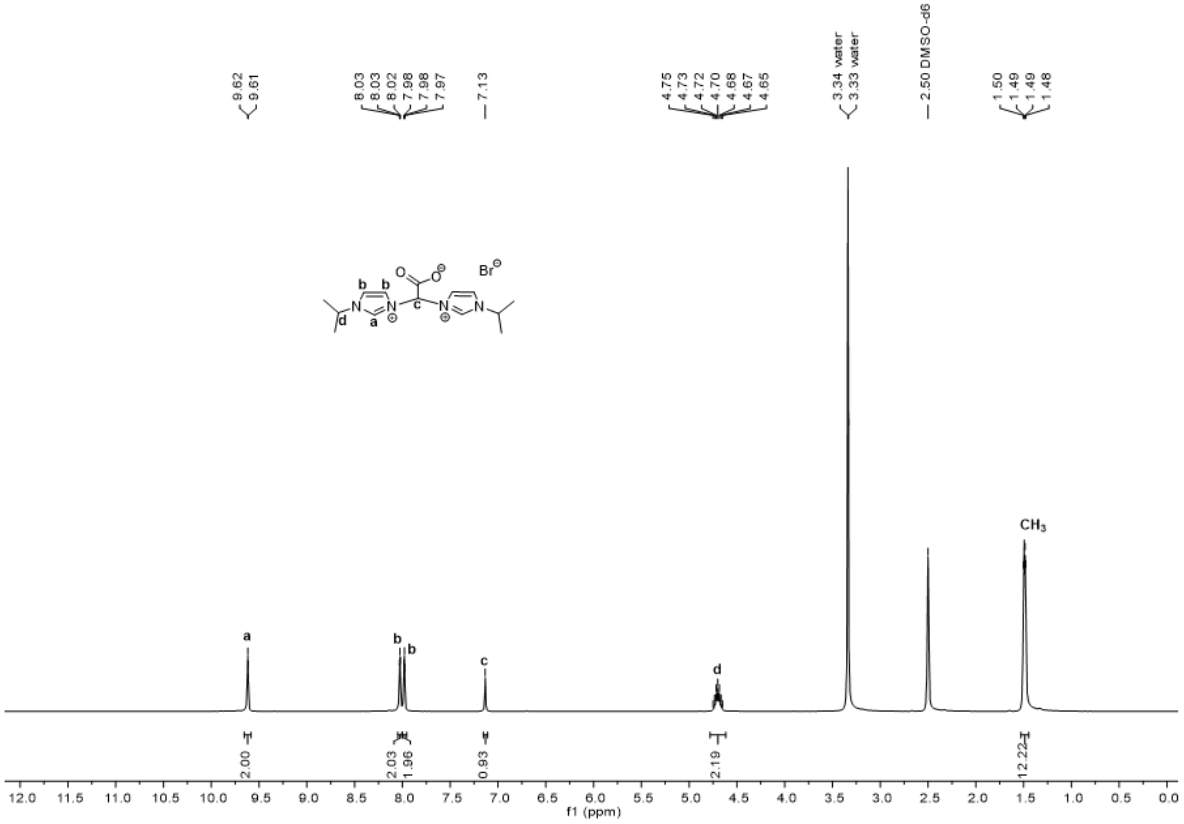

SI-Figure 4: ^{1}H NMR spectrum of **L_b-H_2-Br** in DMSO-d_6 at room temperature.

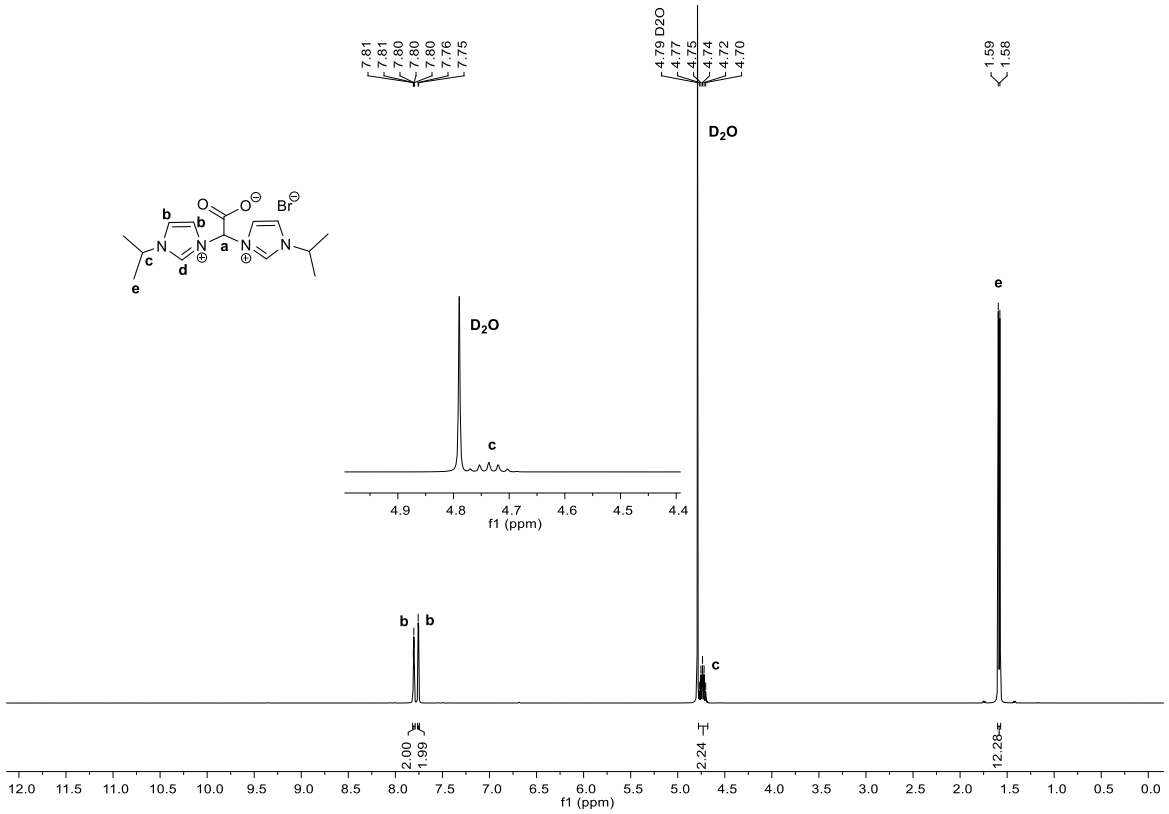

SI-Figure 5: ^{1}H NMR spectrum of **L_b-H_2-Br** in DMSO-d_6 at room temperature.

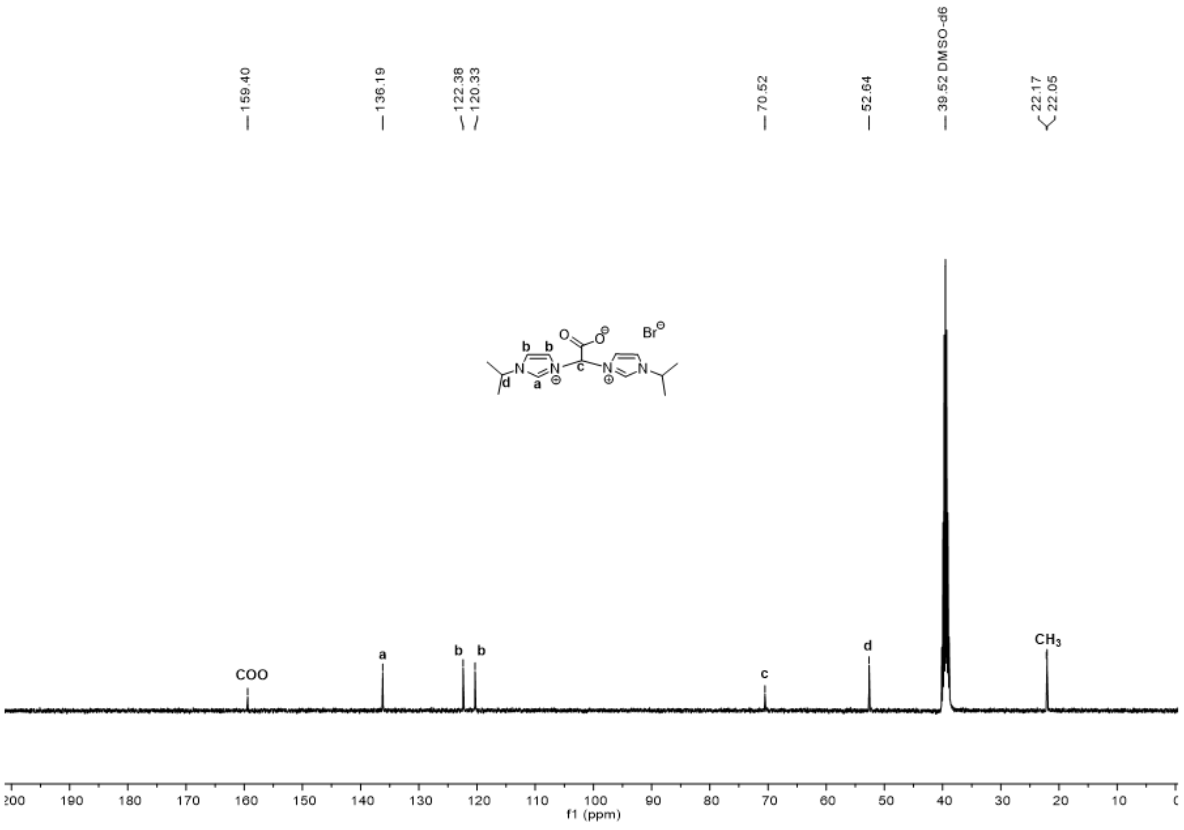

SI-Figure 6: ^{13}C NMR spectrum of **L_b-H_2-Br** in DMSO-d_6 at room temperature.

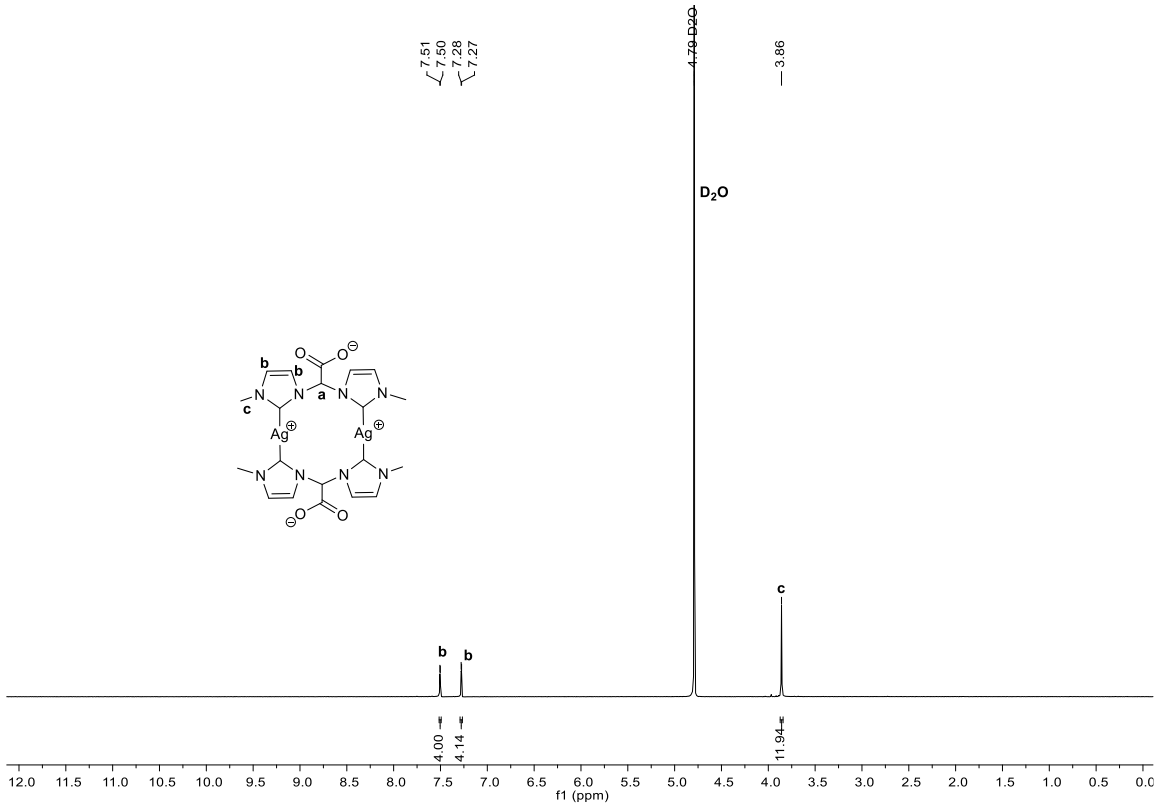

SI-Figure 7: ^{1}H NMR spectrum of **$Ag_2(L_a)_2$** in D_2O at room temperature.

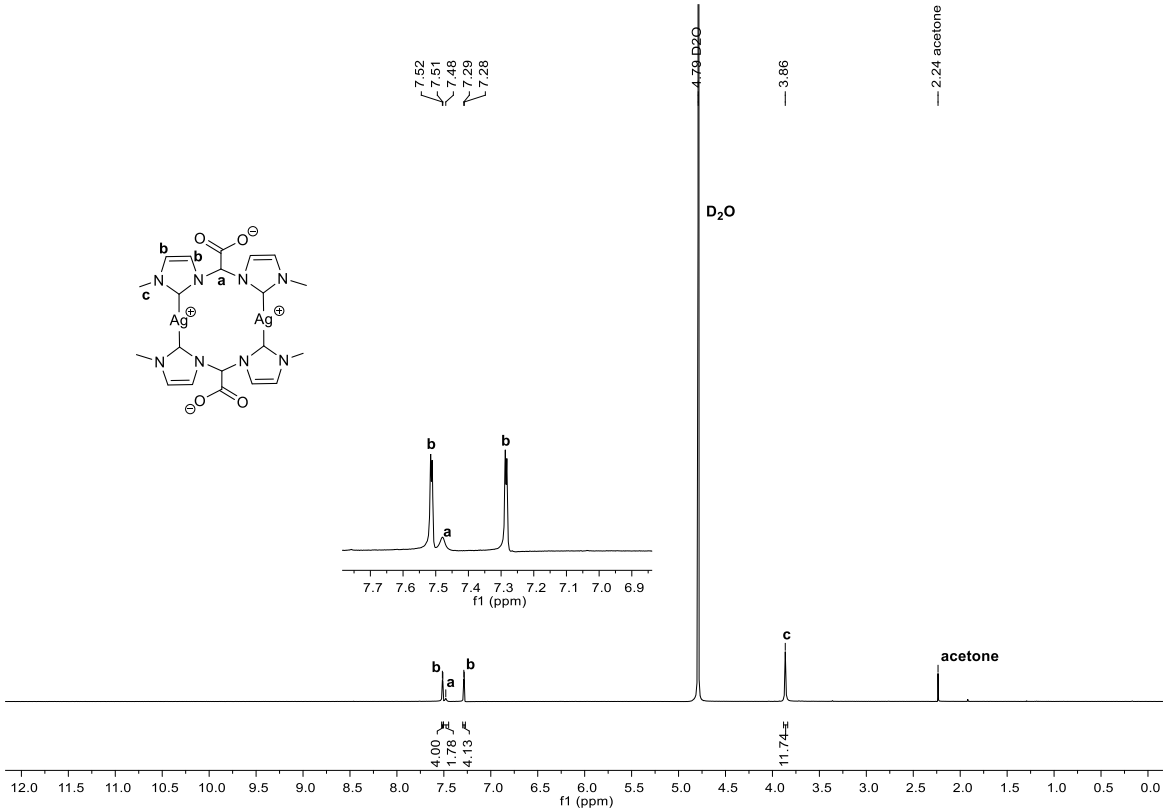

SI-Figure 8: ^{1}H NMR spectrum of **$Ag_2(L_a)_2$** in D_2O at room temperature. Acetone is present, but the methylene bridge proton is visible.

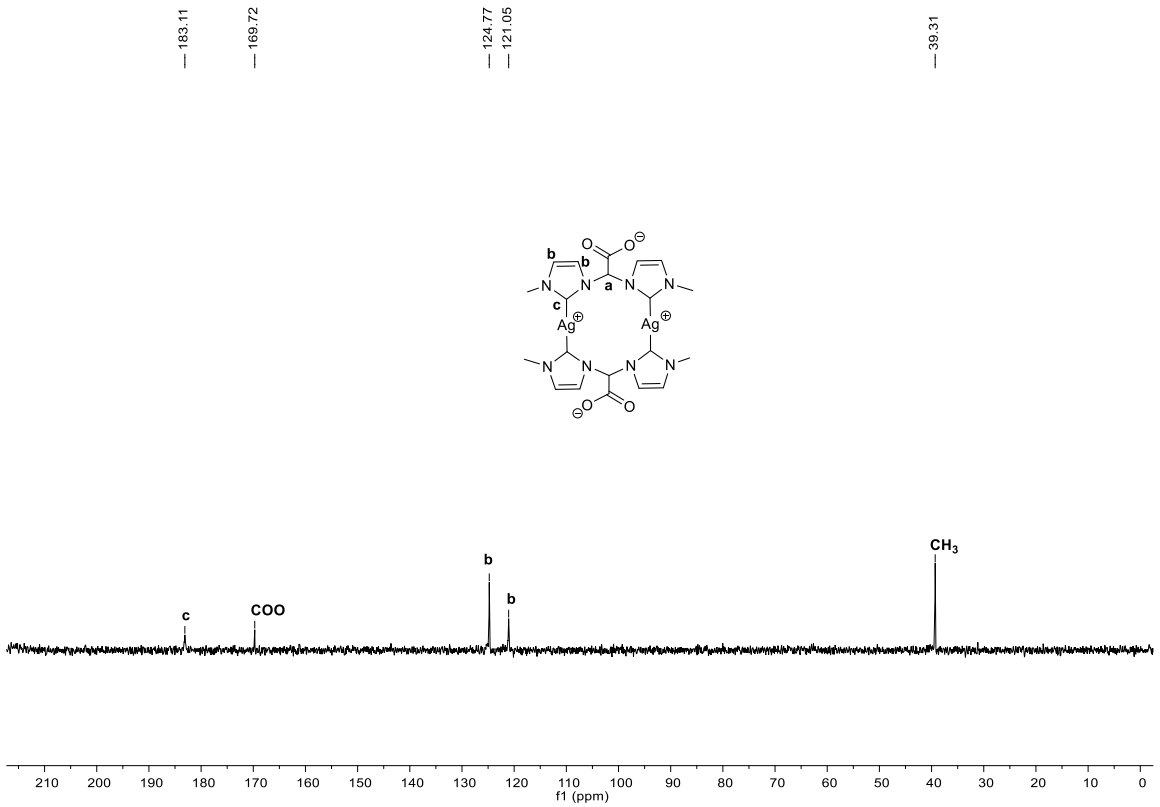

SI-Figure 9: ^{13}C NMR spectrum of **$Ag_2(L_a)_2$** in D_2O at room temperature.

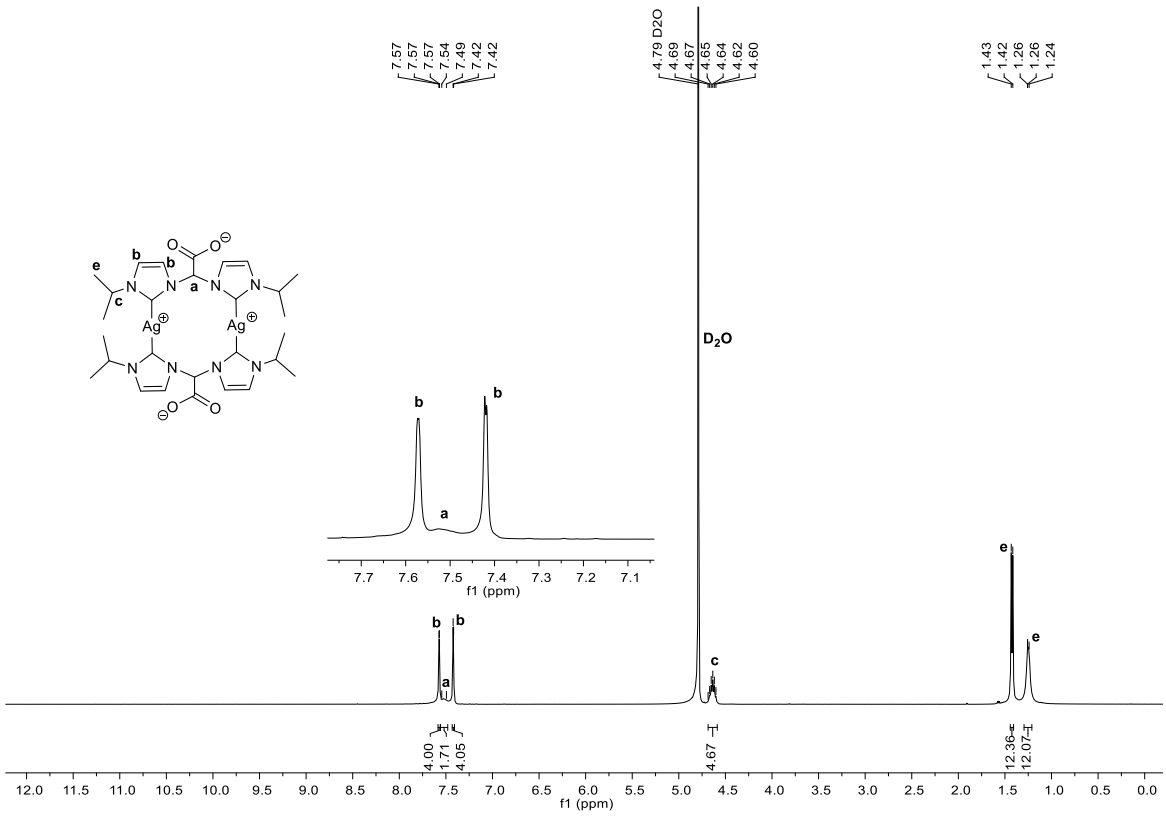

SI-Figure 10: ^{1}H NMR spectrum of **$Ag_2(L_b)_2$** in D^2O at room temperature.

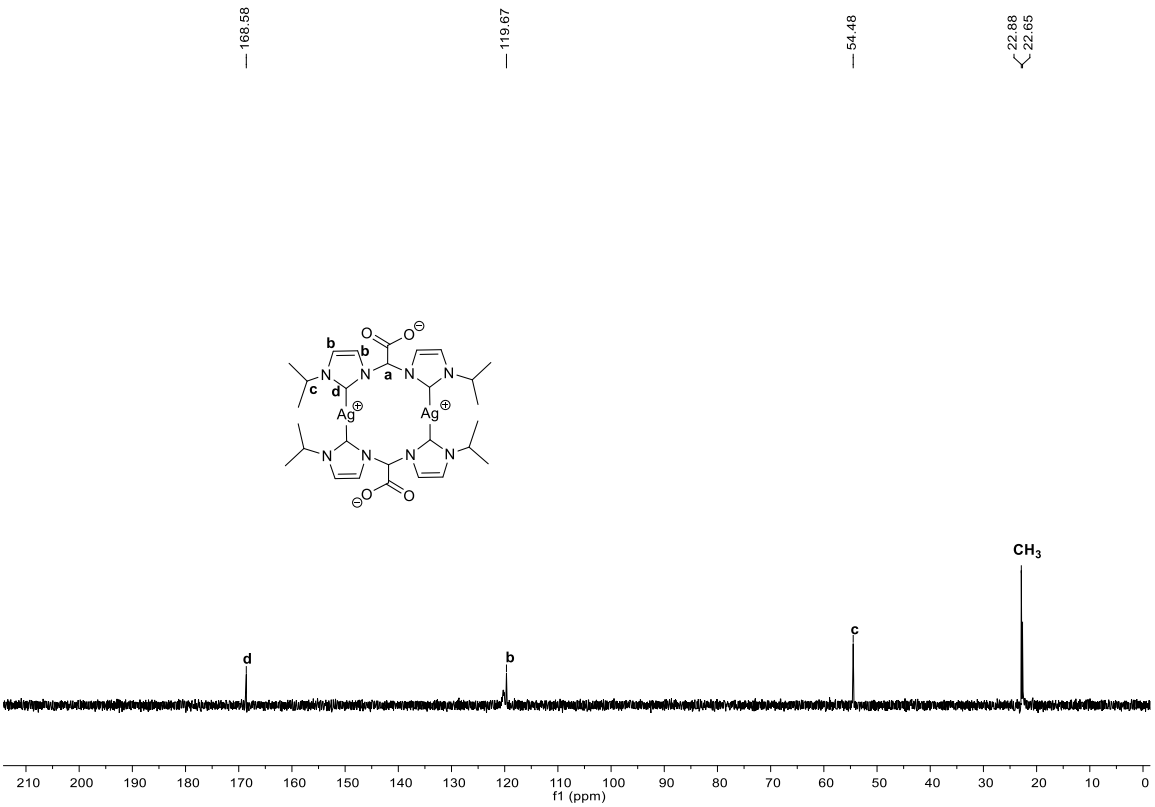

SI-Figure 11: ^{13}C NMR spectrum of **$Ag_2(L_b)_2$** in D_2O at room temperature.

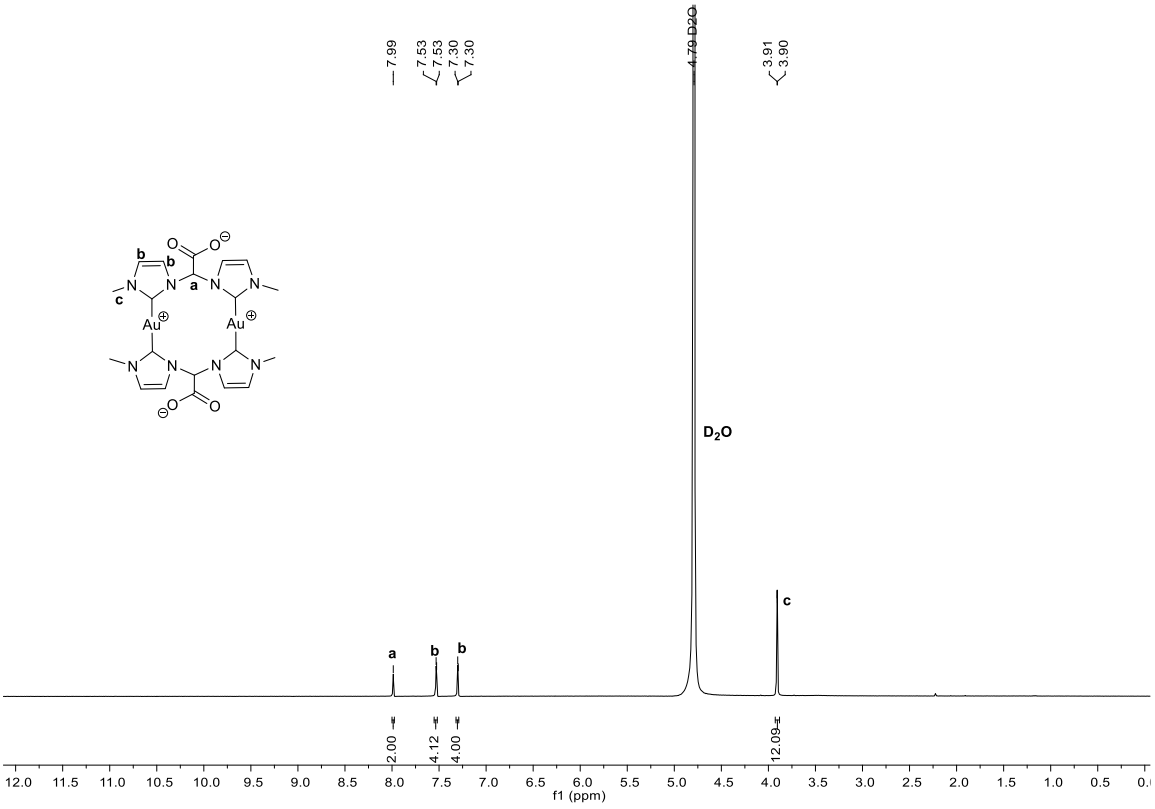

SI-Figure 12: ^{1}H NMR spectrum **$Au_2(L_a)_2$** in D_2O at room temperature.

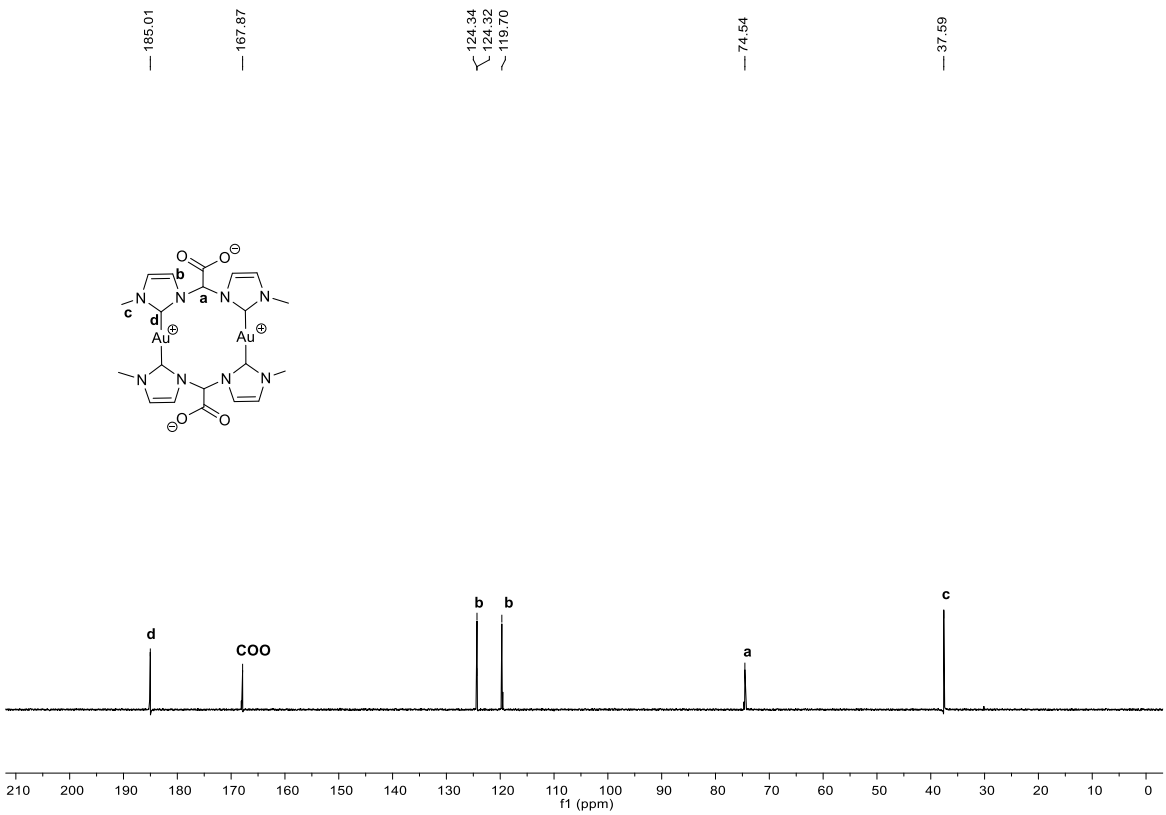

SI-Figure 13: ^{13}C Cryo NMR spectrum of **$Au_2(L_a)_2$** in D_2O at room temperature.

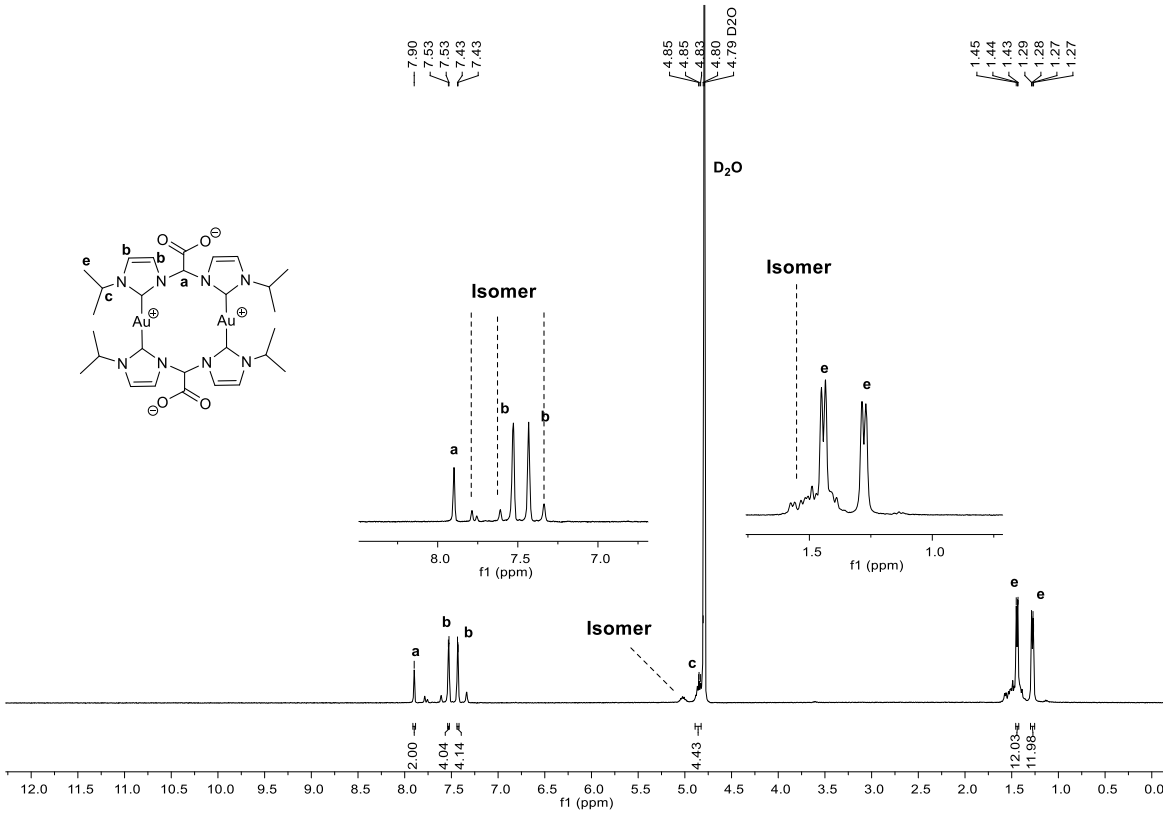

SI-Figure 14: ^{1}H NMR spectrum of isomer mixture of **$Au_2(L_b)_2$** in D_2O at room temperature.

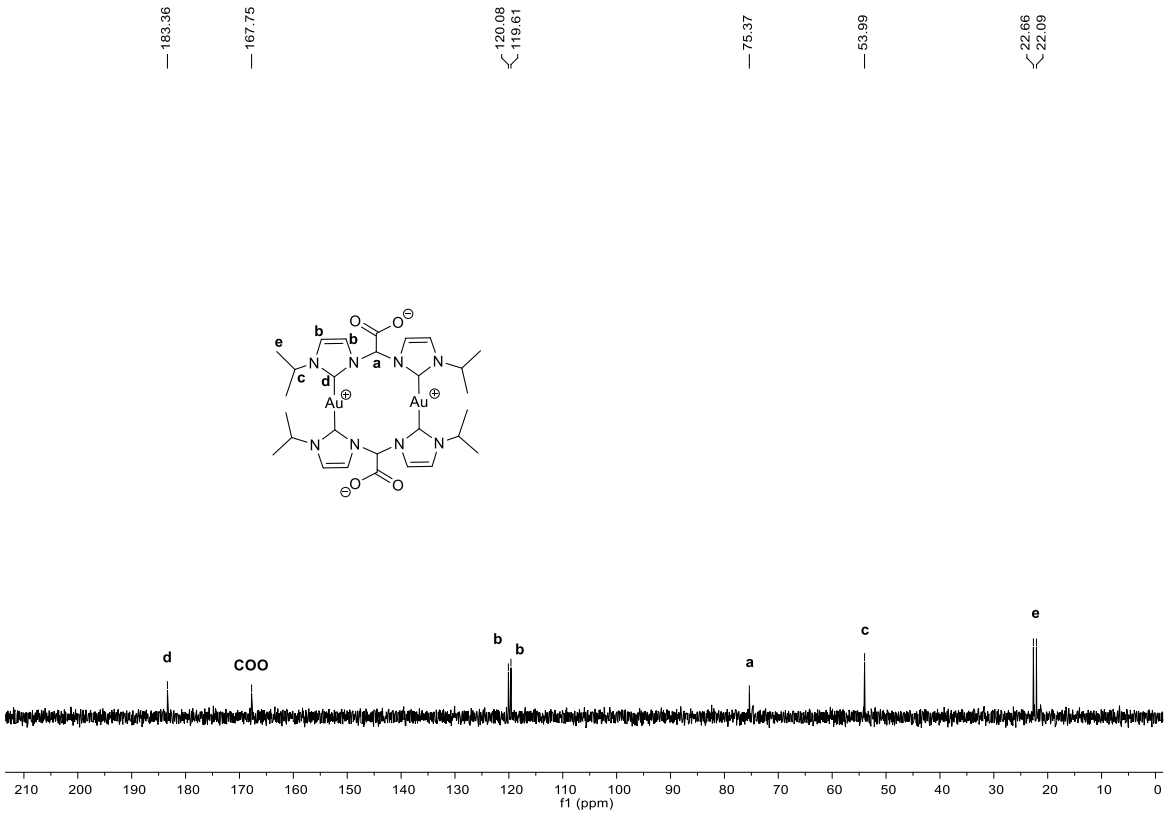

SI-Figure 15: ^{13}C NMR spectrum of isomer mixture of $\mathbf{Au_2(L_b)_2}$ in D_2O at room temperature.

3. DOSY Spectra

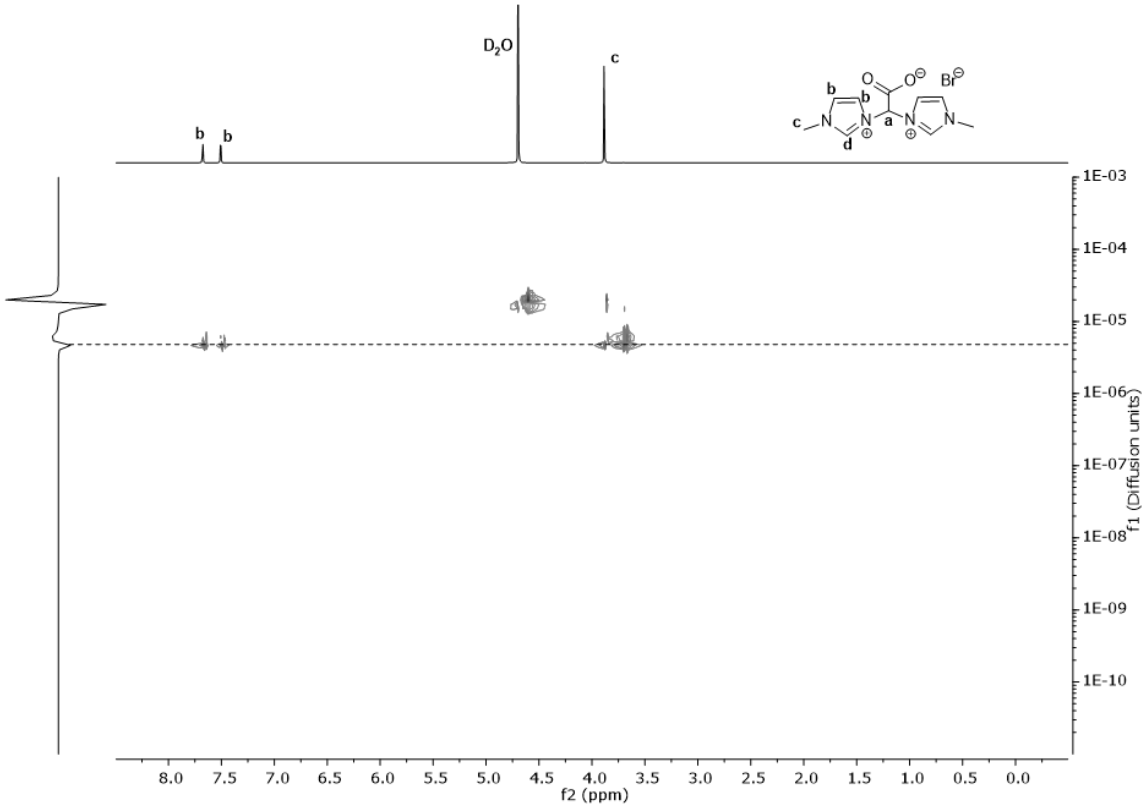

SI-Figure 16: DOSY spectrum of **L_a-H_2-Br** in D_2O at room temperature. Diffusion coefficient amounts to $4.60 \cdot 10^{-06}$ cm^2/s.

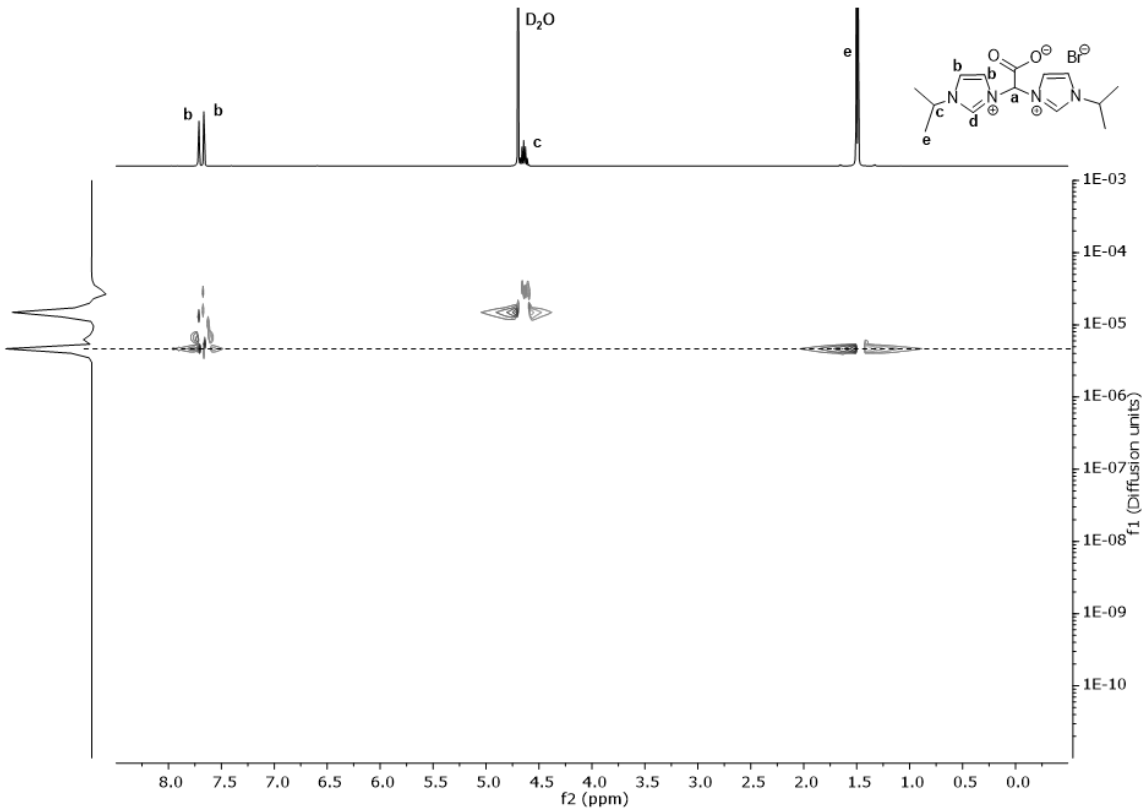

SI-Figure 17: DOSY spectrum of **L_b-H_2-Br** in D_2O at room temperature. Diffusion coefficient amounts to $4.74 \cdot 10^{-06}$ cm^2/s.

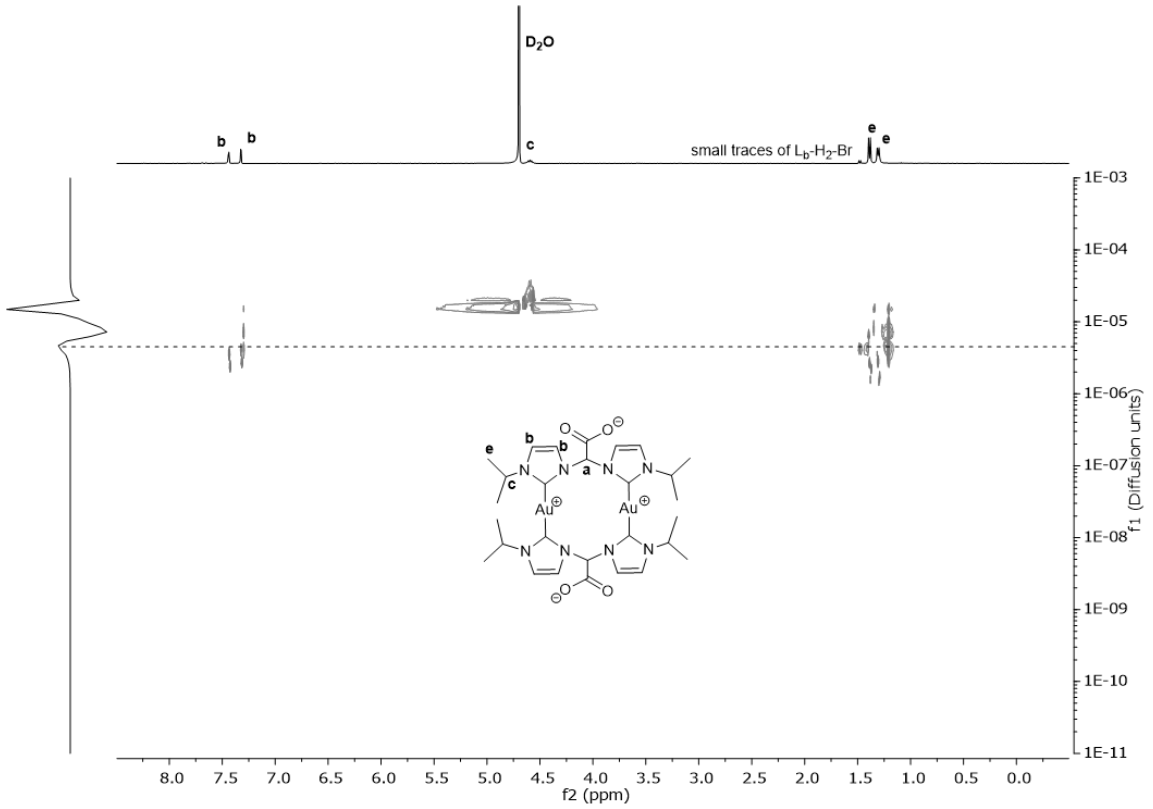

SI-Figure 18: DOSY spectrum of $\mathbf{Ag_2(L_a)_2}$ in D_2O at room temperature. Diffusion coefficient amounts to $4.13 \cdot 10^{-06}$ cm^2/s.

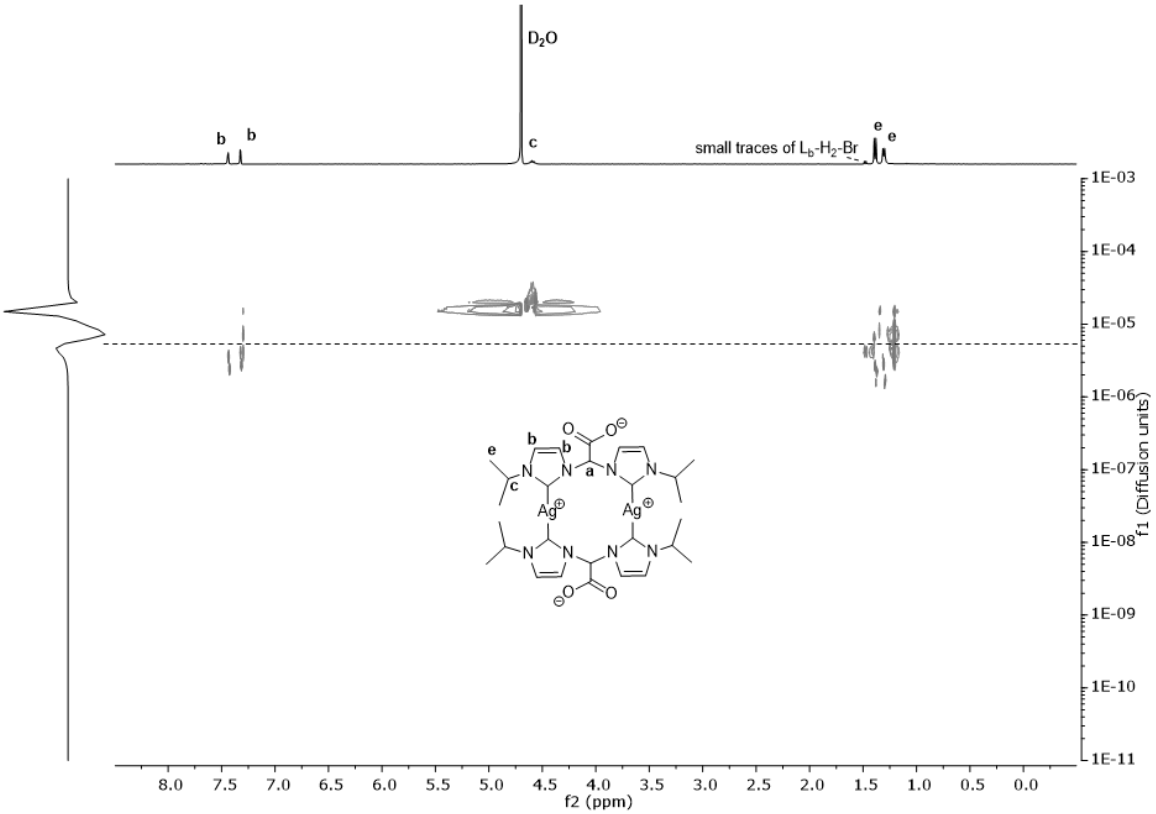

SI-Figure 19: DOSY spectrum of $\mathbf{Ag_2(L_b)_2}$ in D_2O at room temperature. Diffusion coefficient amounts to $4.40 \cdot 10^{-06}$ cm^2/s.

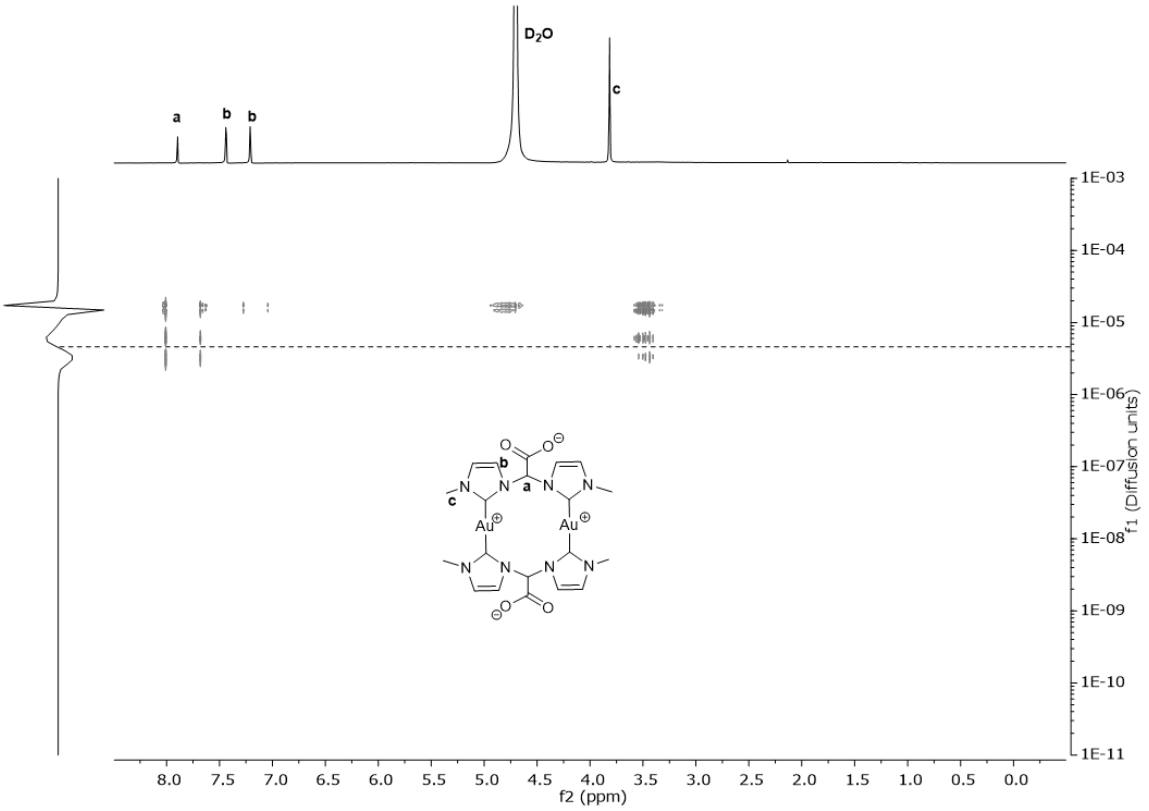

SI-Figure 20: DOSY spectrum of isomer mixture of **$Au_2(L_a)_2$** in D_2O at room temperature. Diffusion coefficient amounts to $4.26 \cdot 10^{-06}$ cm^2/s.

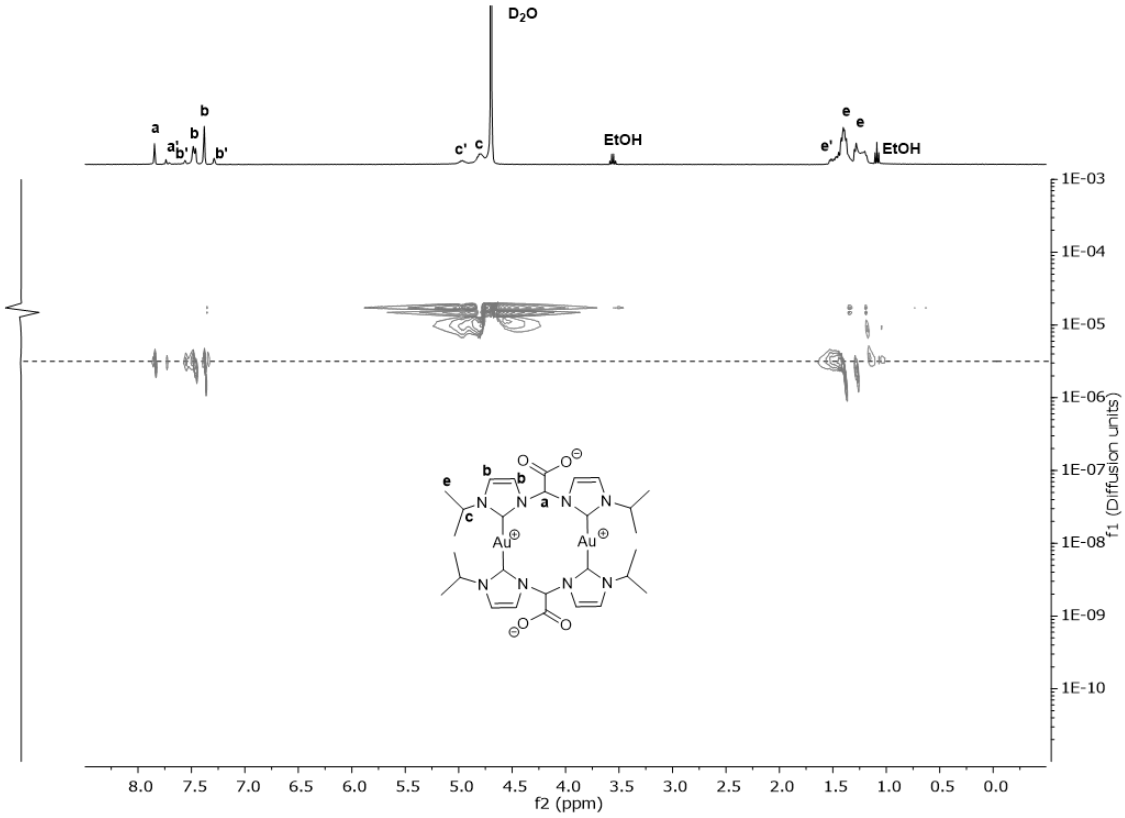

SI-Figure 21: DOSY spectrum of isomer mixture of **$Au_2(L_b)_2$** in D_2O at room temperature. Diffusion coefficient amounts to $4.00 \cdot 10^{-06}$ cm^2/s.

4. VT NMR spectra for decarboxylation studies

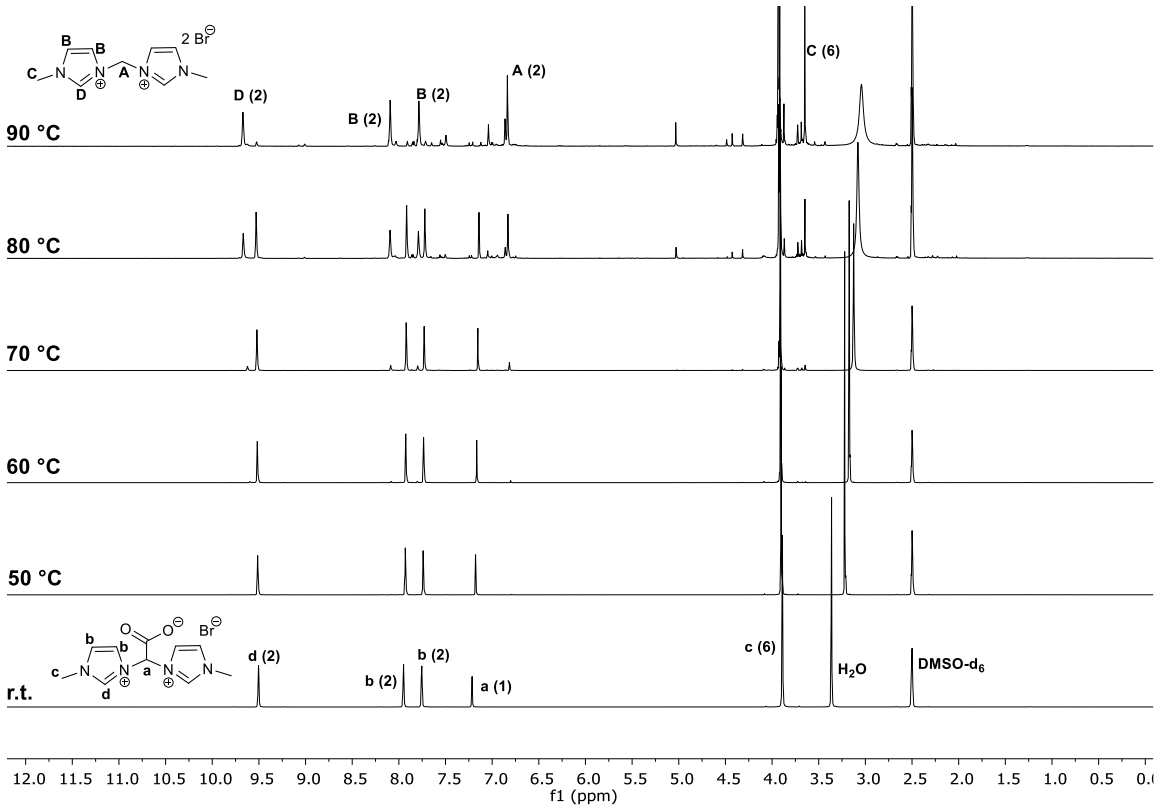

SI-Figure 22: VT(^{1}H)-NMR of **L_a-H_2-Br** in DMSO-d_6 between room temperature (r.t.) and 90 °C. The chemical shifts are assigned with letters and the corresponding integral in brackets.

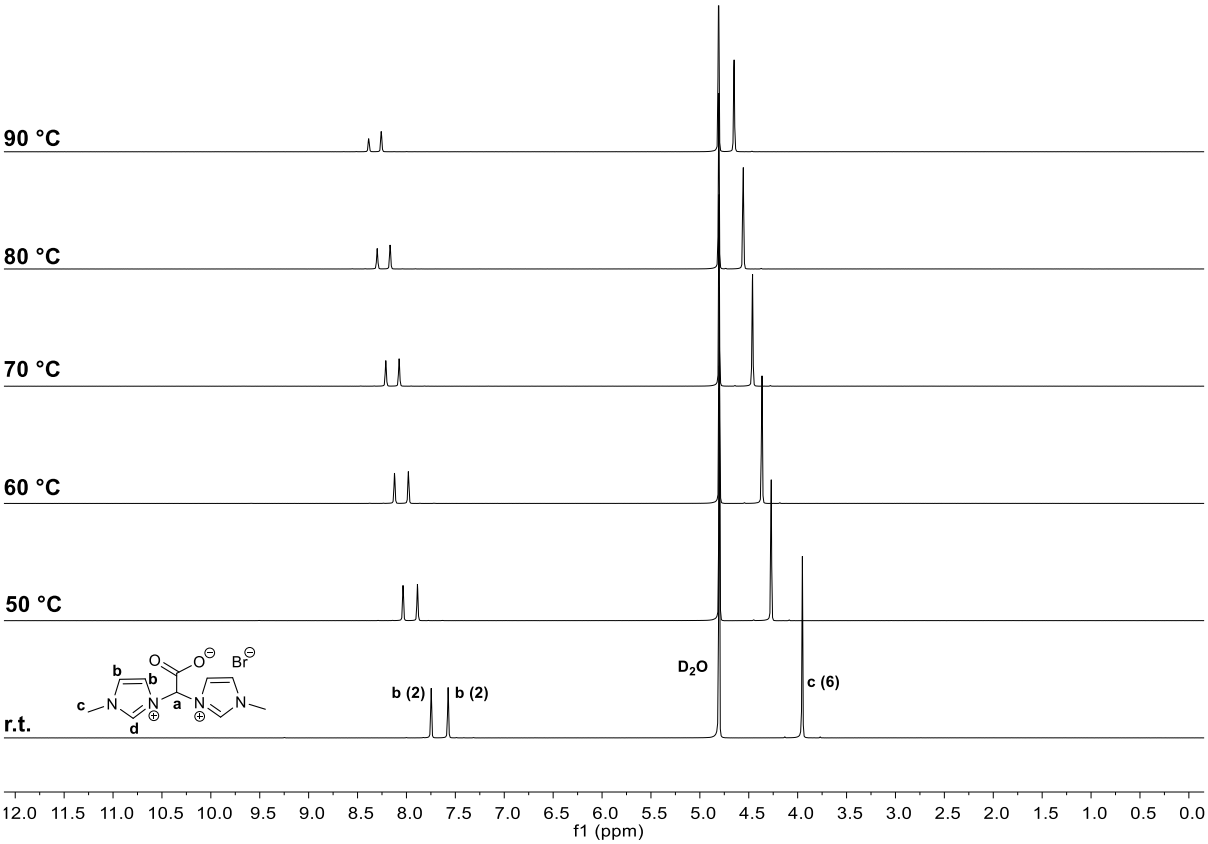

SI-Figure 23: VT(^{1}H)-NMR of **L_a-H_2-Br** in D_2O between room temperature (r.t.) and 90 °C. The chemical shifts are assigned with letters and the corresponding integral in brackets.

5. Protonation Studies

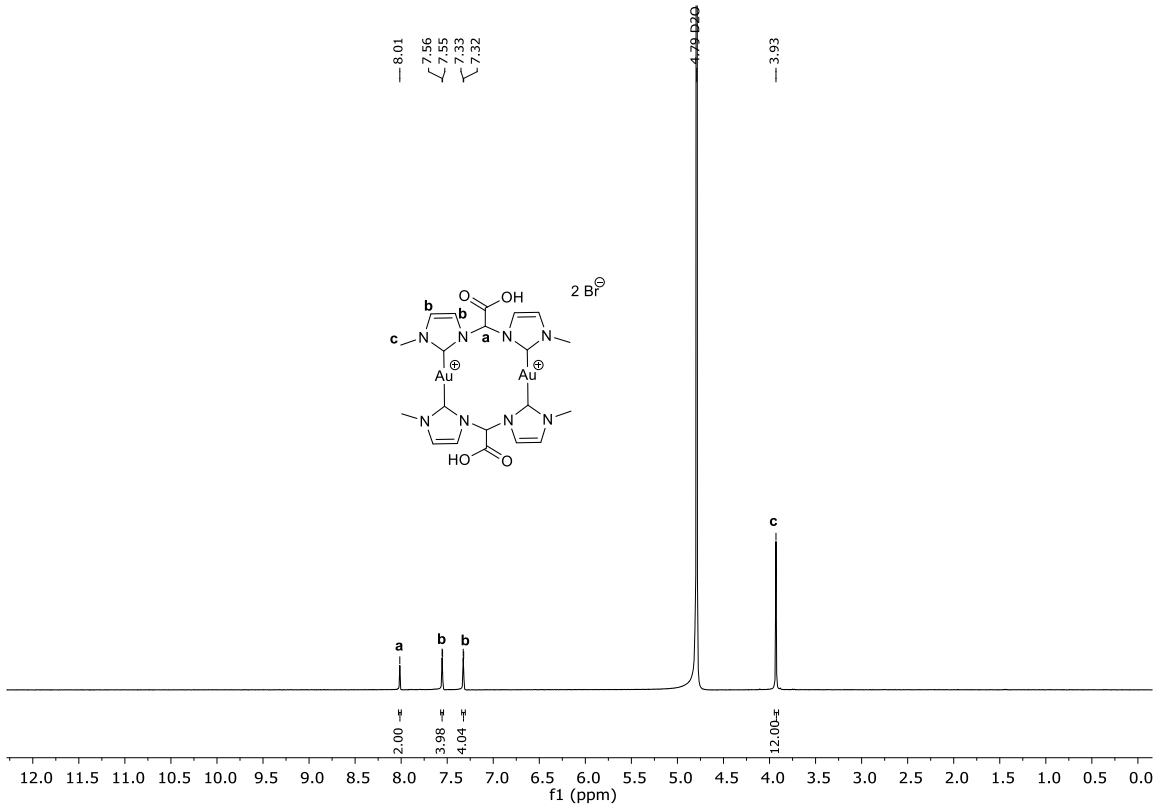

SI-Figure 24: ^{1}H NMR spectrum of **$Au_2(L_a)_2(HBr)_2$** in D_2O at room temperature.

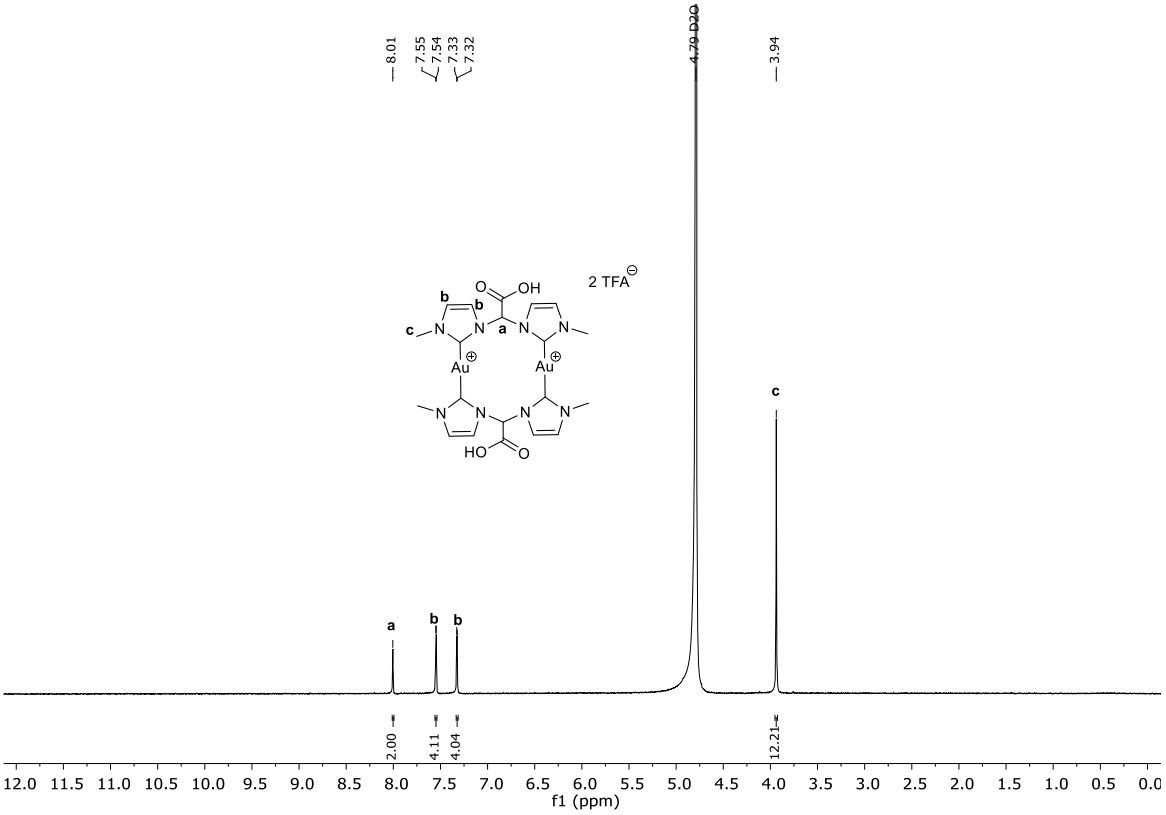

SI-Figure 25: ^{1}H NMR spectrum of **$Au_2(L_a)_2(HTFA)_2$** in D_2O at room temperature.

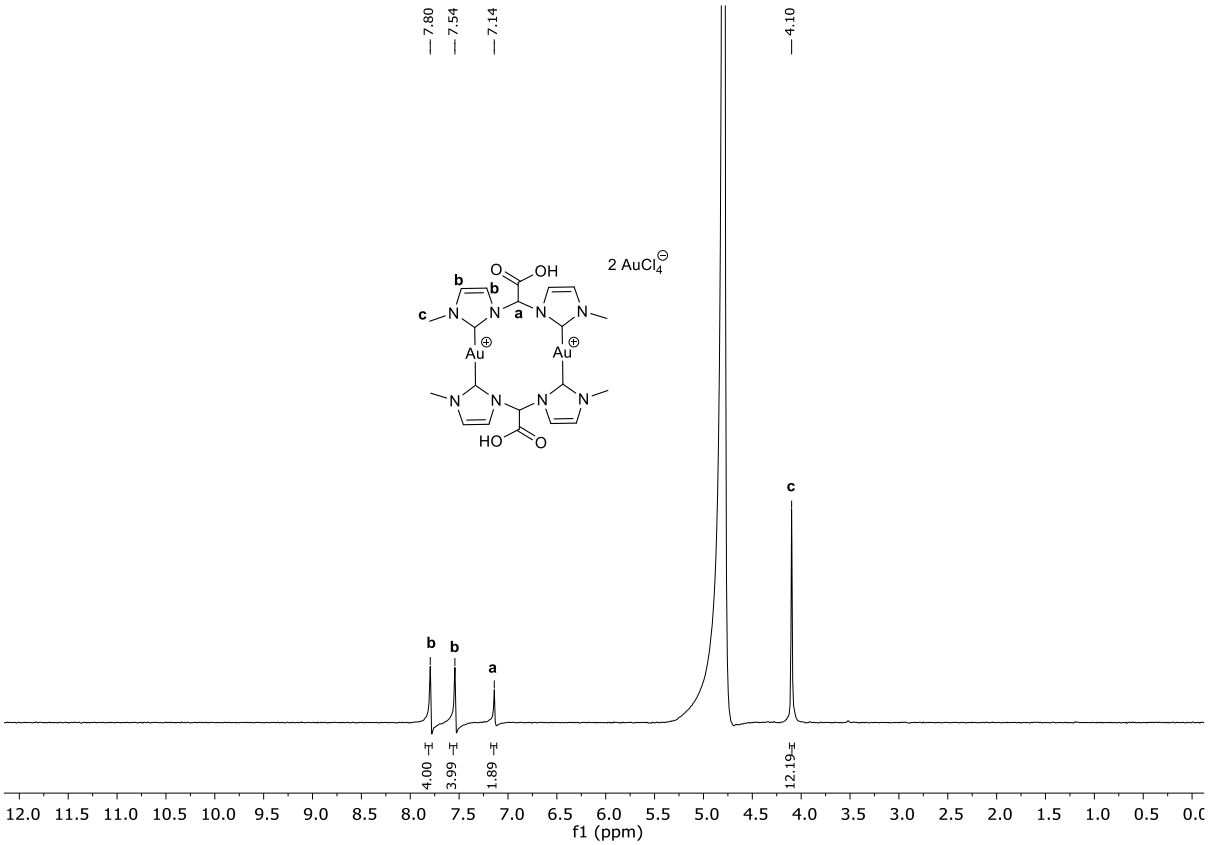

SI-Figure 26: ^{1}H NMR spectrum of **$Au_2(L_a)_2(HAuCl_4)_2$** in D_2O at room temperature.

6. Esterification and Amidation attempts

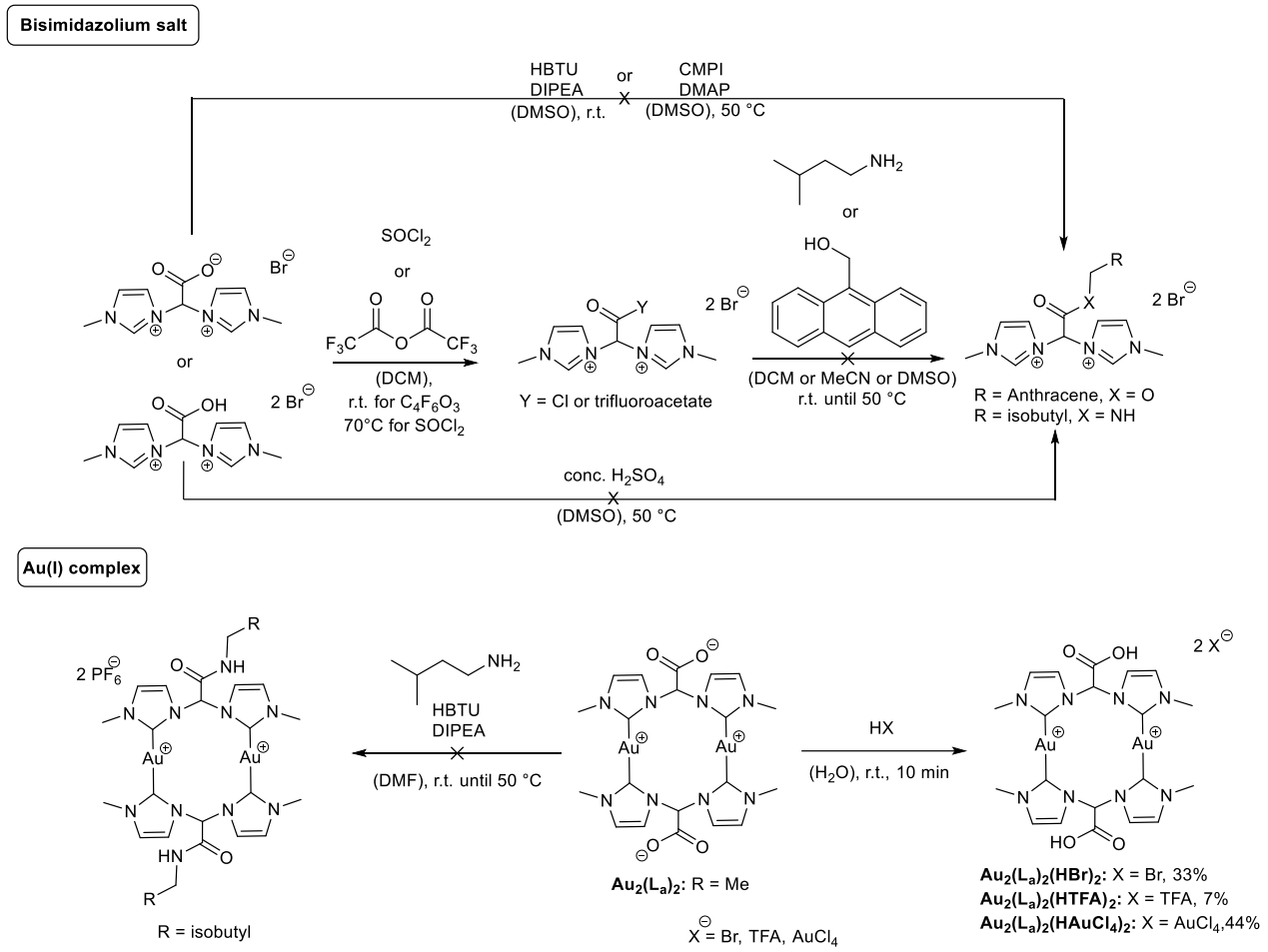

SI-Scheme 1: Reactivity studies of bisimidazolium salt L_a-H_2-Br or the gold(I) complex $Au_2(L_a)_2$ towards protonation, esterification or amidation reactions. HBTU = 3-[Bis(dimethyl-amino)methyliumyl]-3H-benzotriazol-1-oxide-hexafluorphosphate, DIPEA = N-Ethyl-N-(propan-2-yl)propan-2-amine, CMPI = 2-Chlor-1-methylpyridiniumiodide, DMAP = 4-Di-methylaminopyridine.

7. FT-IR spectra

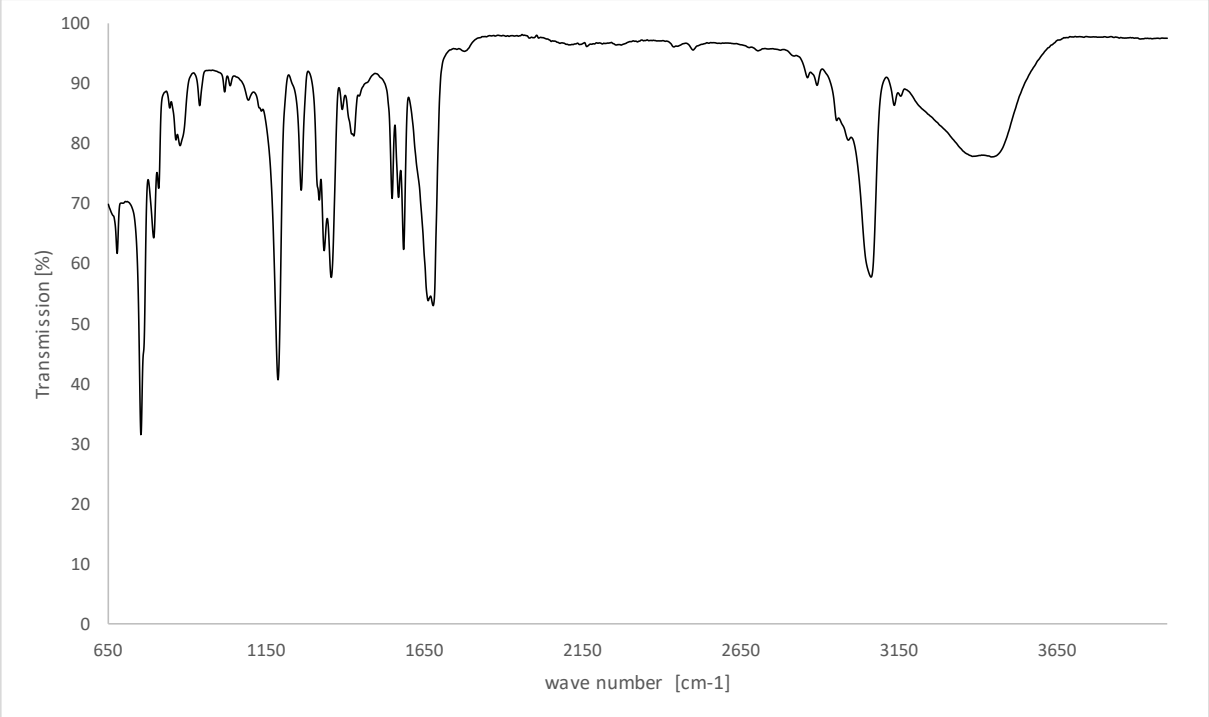

SI-Figure 27: FT-IR spectrum of **L_a-H_2-Br**.

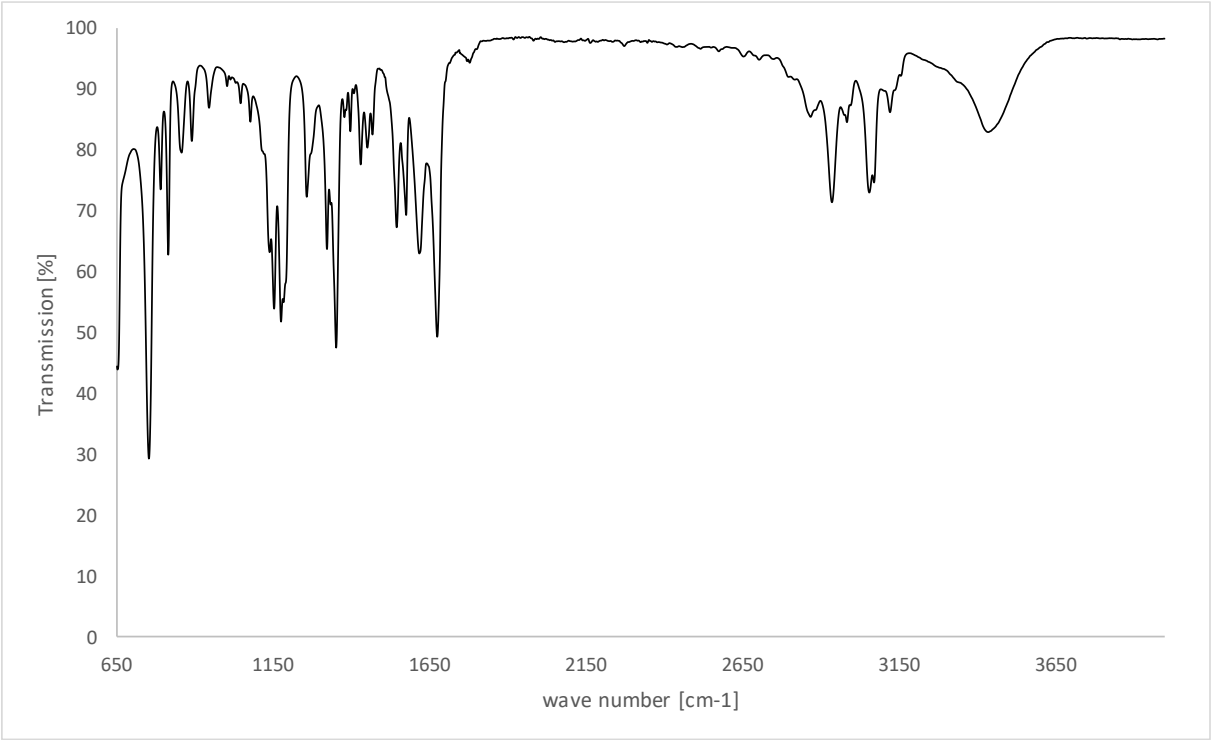

SI-Figure 28: FT-IR spectrum of **L_b-H_2-Br**.

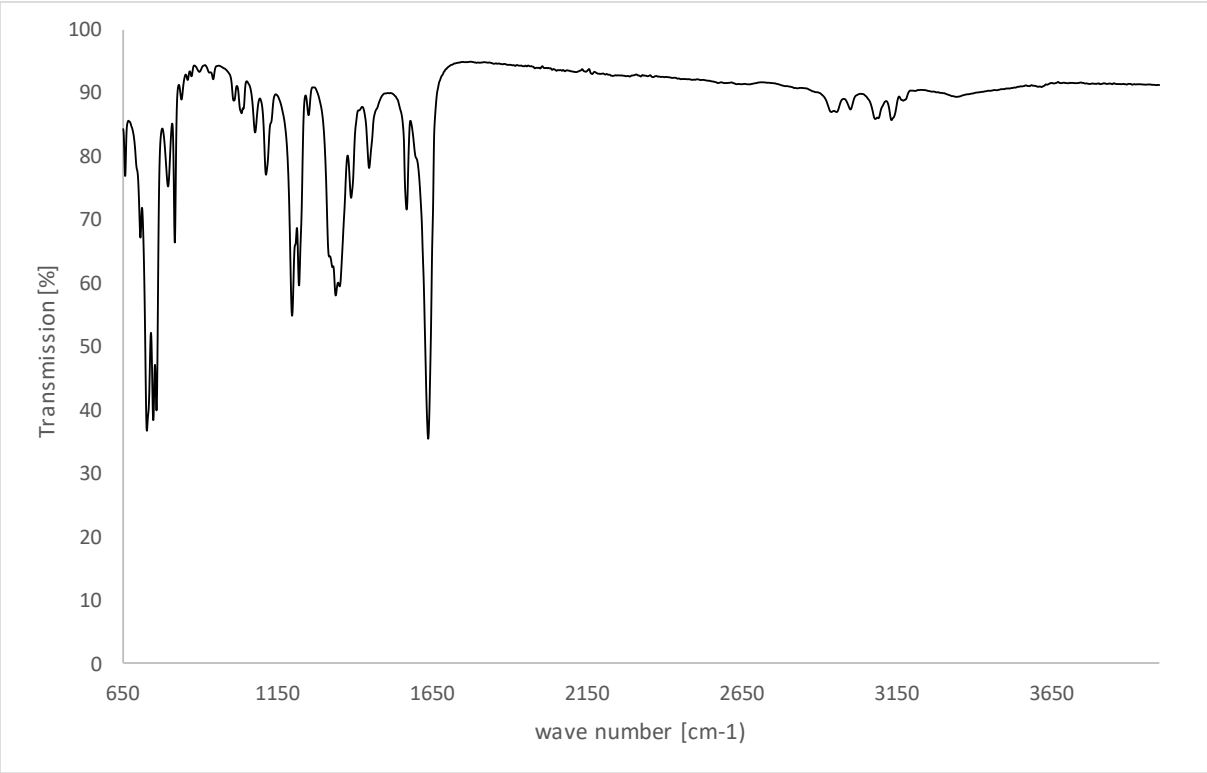

SI-Figure 29: FT-IR spectrum of **$Ag_2(L_a)_2$**.

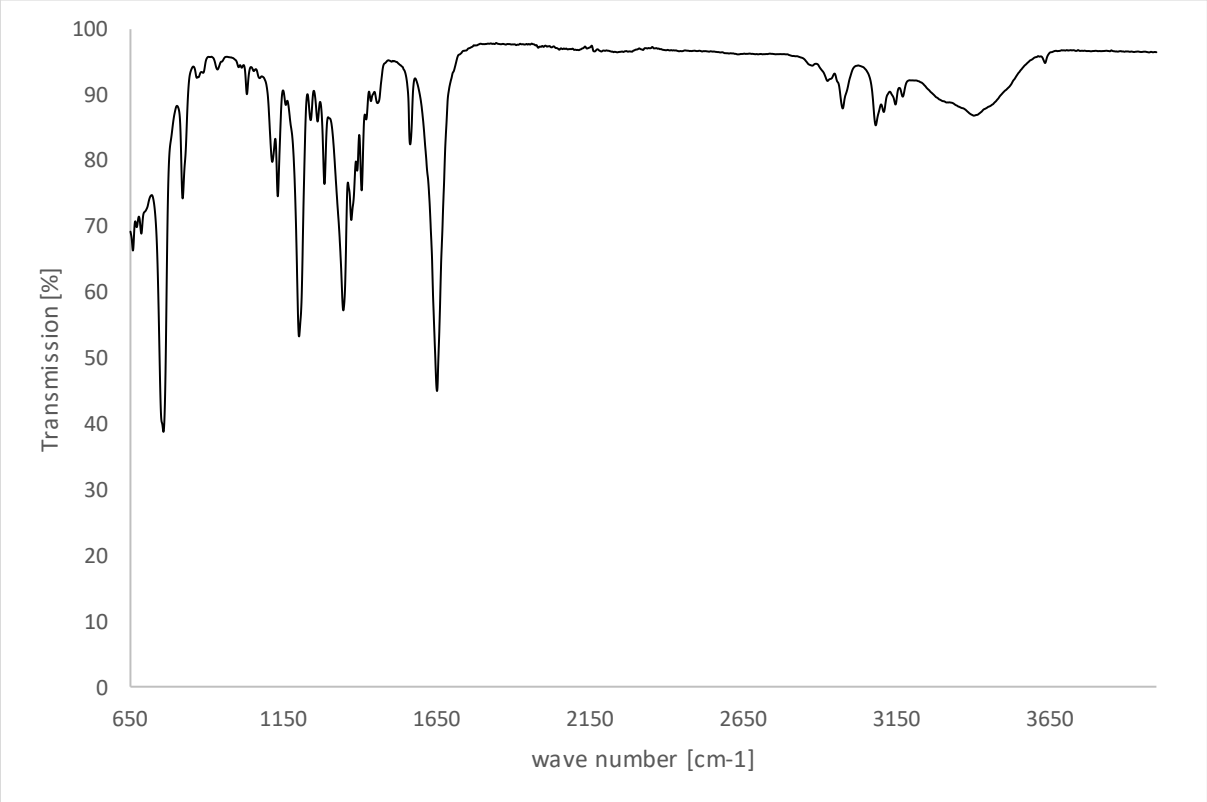

SI-Figure 30: FT-IR spectrum of **$Ag_2(L_b)_2$**.

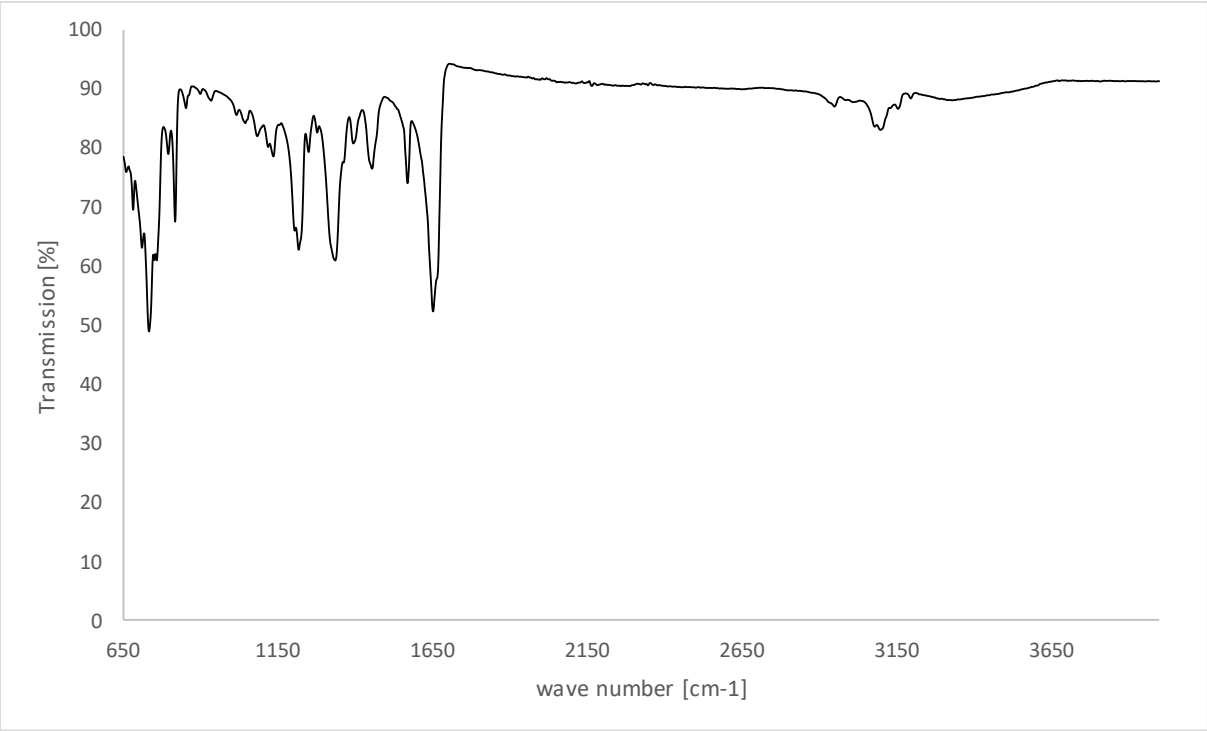

SI-Figure 31: FT-IR spectrum of **$Au_2(L_a)_2$**.

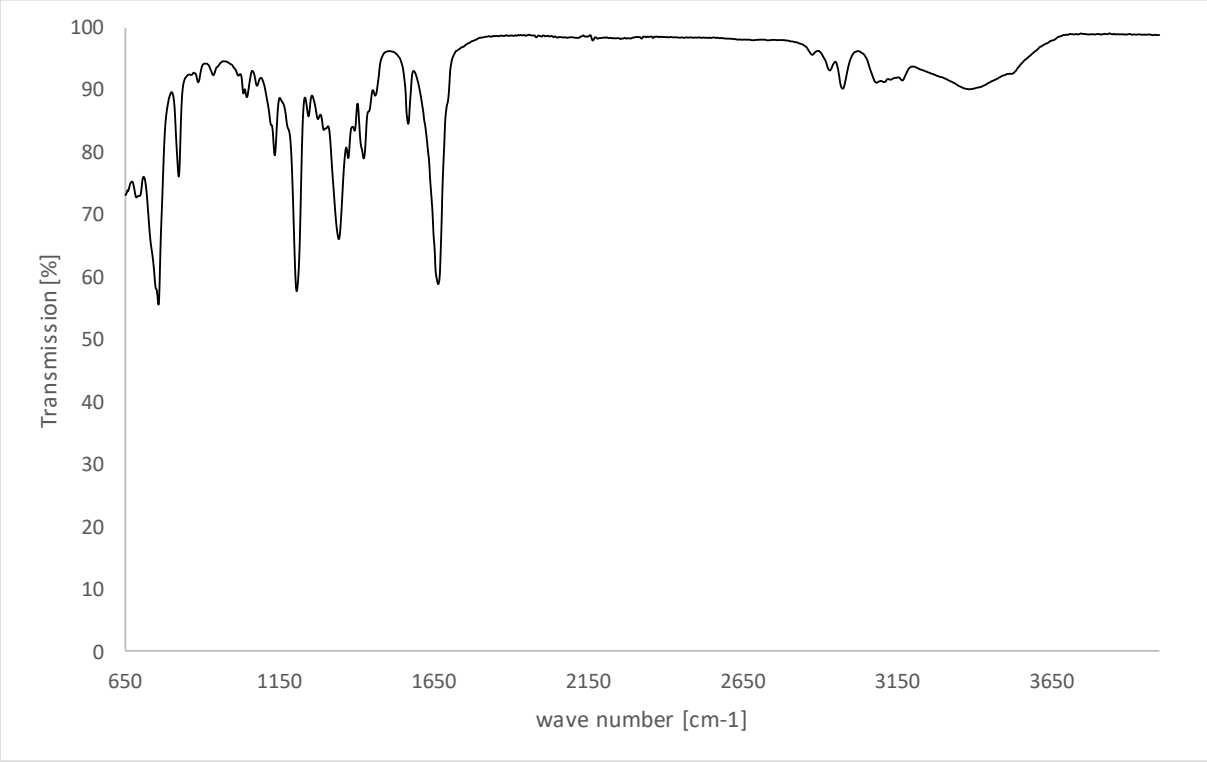

SI-Figure 32: FT-IR spectrum of **$Au_2(L_b)_2$**.

8. SC-XRD Data

Table 1:Crystallographic details of **L_a-H_2-PF_6**, **$Ag_2(L_a)_2$**, **$Ag_2(L_b)_2$** and **$Au_2(L_a)_2$**.

	L_a-H_2-PF_6 (CCDC 1942899)	**$Ag_2(L_a)_2$** (CCDC 1942902)	**$Ag_2(L_b)_2$** (CCDC 1942901)	**$Au_2(L_a)_2$** (CCDC 1942900)
formula	$C_{10}H_{19}F_6N_4O_5P$	$C_{20}H_{22}Ag_2N_8O_4$	$C_{28}H_{38}Ag_2N_8O_4$	$C_{20}H_{22}Au_2N_8O_4$
formula weight	420.26	654.18	766.40	832.38
color/habit	Clear pale yellow fragment	Clear colorless fragment	Clear colorless fragment	Clear colorless fragment
crystal dimensions [mm^3]	0.08 x 0.081 x 0.12	0.082 x 0.133 x 0.146	0.078 x 0.149 x 0.361	0.041 x 0.138 x 0.167
crystal system	monoclinic	triclinic	triclinic	monoclinic
space group	$P\,2_1/n$	$P\,\bar{1}$	$P\,\bar{1}$	$C\,2/m$
a [Å]	11.4241(3)	11.3434(5)	8.2043(6)	15.6805(11)
b [Å]	6.2939(2)	12.6516(5)	11.6334(7)	21.4574(13)
c [Å]	23.5348(7)	12.7157(6)	12.2004(8)	12.2321(8)
α [deg]	90	107.761(2)	100.631(3)	90
β [deg]	94.120(0)	99.703(2)	90.414(3)	126.911(3)
γ [deg]	90	113.659(2)	91.170(3)	90
V [$Å^3$]	1687.83(9)	1500.65(12)	1144.16(13)	3290.7(4)
Z	4	2	2	8
T [K]	123(2)	100(2)	100(2)	123(2)
D_{calcd} [g/cm^{-3}]	1.654	1.448	1.397	1.991
μ [mm^{-1}]	0.258	1.339	0.909	8.970
F(000)	864	648	492	1872
θ range [deg]	1.93 to 25.35	2.24 to 27.45	2.22 to 25.02	1.88 to 25.35
index range (h, k, l)	−13 ≤ h ≤ +13 −7 ≤ k ≤ +7 −28 ≤ l ≤+28	−14 ≤ h ≤ +14 −16 ≤ k ≤ +16 −16 ≤ l ≤+16	−9 ≤ h ≤ +9 −13 ≤ k ≤ +13 −14 ≤ l ≤+14	−12 ≤ h ≤ +18 0 ≤ k ≤ +25 −14 ≤ l ≤+14
Reflections collected	31974	107428	19315	2859
no. of indep reflns/R_{int}	3103/0.0518	6857/0.0554	4051/0.0473	2589/0
No. of obsd reflns (*I*>2σ(I))	2521	6017	3702	2090
no. of data/ restraints/params	3103/0/261	6857/0/311	4051/78/282	2859/87/239
R1/wR2 (*I*>2σ(I))	0.0330/0.0682	0.0226/0.0459	0.0224/0.0589	0.0294/0.0572
R1/wR2 (*all data*)	0.0470/0.0737	0.0293/0.0477	0.0289/0.0634	0.0463/0.0590
GOF (on F^2)	1.039	1.054	1.042	0.832
Largest diff peak and hole [e $Å^{-3}$]	0.286 and -0.312	0.431 and -0.555	0.656 and -0.680	1.188 and -1.253

9. References

1. R. Puerta-Oteo, M. Hölscher, M. V. Jiménez, W. Leitner, V. Passarelli, J. J. Pérez-Torrente, *Organometallics*, 2018, **37**, 684-696.
2. Y. Li, B. Dominelli, R. M. Reich, B. Liu, F. E. Kühn, *Catal. Commun.*, 2019, **124**, 118-122.
3. J. Rieb, B. Dominelli, D. Mayer, C. Jandl, J. Drechsel, W. Heydenreuter, S. A. Sieber, F. E. Kühn, *Dalton Trans.*, 2017, **46**, 2722-2735.
4. J. Cure, R. Poteau, I. C. Gerber, H. Gornitzka, C. Hemmert, *Organometallics*, 2012, **31**, 619-626.
5. *APEX suite of crystallographic software*, APEX 2, Version 2014.9-0 and APEX 3, Version 2015-5.2, Bruker AXS Inc., Madison, Wisconsin, USA, 2014/2015.
6. *SAINT*, Versions 8.32B, 8.34A and 8.38A, Bruker AXS Inc., Madison, Wisconsin, USA, 2012/2014/2017.
7. *SADABS*, Versions 2012/1, 2014/5 and 2016/2 and *TWINABS*, Version 2012/1, Bruker AXS Inc., Madison, Wisconsin, USA, 2012/2014/2016.
8. G. M. Sheldrick, *Acta Crystallogr. Sect. A*, 2015, **71**, 3–8.
9. G. M. Sheldrick, *Acta Crystallogr. Sect. C*, 2015, **71**, 3–8.
10. C. B. Hübschle, G. M. Sheldrick, B. Dittrich, *J. Appl. Cryst.*, 2011, **44**, 1281–1284
11. *International Tables for Crystallography, Vol. C* (Ed.: A. J. Wilson), Kluwer Academic Publishers, Dordrecht, The Netherlands, 1992, Tables 6.1.1.4 (pp. 500–502), 4.2.6.8 (pp. 219–222), and 4.2.4.2 (pp. 193–199).
12. A.L. Spek, *Acta Crystallogr. Sect. C*, 2015, **71**, 9–18.
13. A. L. Spek, *Acta Crystallogr. Sect. D*, 2009, **65**, 148–155.
14. C. F. Macrae, I. J. Bruno, J. A. Chisholm, P. R. Edgington, P. McCabe, E. Pidcock, L. Rodriguez-Monge, R. Taylor, J. van de Streek, P. A. Wood, J. Appl. Cryst., 2008, **41**, 466–470.